

00

Department of Physics
University of New York
100 University Street
New York, NY 10003, USA
Tel: 1-212-850-2576
1-212-850-2507

International Journal of Modern Physics B, Vol. 10, No. 15 (1996) 1821-1862
© World Scientific Publishing Company

Department of Physics
Tsing Hua University
101, Sec. 2, Kuang-Fu Rd.
Taipei, TAIWAN
Tel: 886-35-715928
886-35-723052
hcku@phys.nthu.edu.tw

Department of Physics
University of Utah
115 S. 1400 E.
Salt Lake City, UT 84112, USA
Tel/Fax: 1-801-3633444
mattis@mail.physics.utah.edu

CLUES TO THE EXISTENCE OF DETERMINISTIC CHAOS IN RIVER FLOW

AMILCARE PORPORATO and LUCA RIDOLFI

*Department of Hydraulics, Transports and Civil Infrastructures,
Polytechnic of Turin, Italy*

Received 21 December 1995

Department of Patras
Department of Engineering
Engineering Science Department
26500 Patras, GREECE
Tel: 30-61-997222
30-61-997255

Department of Mechanical and Structural
Engineering
Department of Science
560012, INDIA
Tel: 91-80-340580
91-80-341683
sarrao@sscu.iisc.ernet.in

ENSI
Ecole Nationale Supérieure de
Techniques de l'Industrie
Chimique
37000 Le Mans Cedex, FRANCE
Tel: 33-31-951212
33-31-951600
sarrao@FRCPNIBITNET

Department of Electrical
and Electronics Engineering
Department of Technology
Saitama
338-8501, JAPAN
Tel: 0480-344111 ext 687
0480-342941

Department of Materials Research
Department of Physics
Sendai 980, JAPAN
Tel: 81-22-2152005
81-22-2152006
schiki@tachp.imr.tohoku.ac.jp

Watson Research Center
218
Route 9W, Yorktown Heights, NY 10598, USA
Tel: 1-914-9452141
suei@yktvmv

Department of Physics
Department of Physics
Academy of Sciences
100080, Beijing, CHINA
Tel: 86-1-2569220
86-1-2568834
HAOZX@thevx.slac.stanford.edu

The present work investigates the existence of a component of deterministic chaos in the discharge time series of a river. The first part of the work is concerned with the reconstruction of the attractor and the calculation of the correlation integral; in the second part the analysis is conducted with the aid of nonlinear prediction. Some clues emerge as to the possible presence of chaos, probably immersed in a phenomenon altogether more extensive and manifold. If confirmed, this presence could provide interesting openings for a better comprehension of the formation mechanism of river flow, and a more precise forecasting of floods.

1. Introduction

Recent developments in the theory of nonlinear dynamical systems have shed new light on the comprehension of complex dynamical systems. In particular, the application of nonlinear methods to time series of natural systems has certainly enhanced the comprehension of phenomena, even though its results are much more "vague" than those obtained by analytical models or laboratory experiments. In such a case, indeed, it is not possible to be completely certain of the presence of deterministic chaos.^{34,71} Because of both the great complexity of these systems, and the fact that the available data for natural phenomenon is often small and contaminated by disturbances of various types, the approach adopted in this case must be different. In accord with the strategy proposed by Grassberger, Schreiber and Schaffrath,³⁴ emphasis is to be placed not on the search of the strongest form of determinism (that is, the absence of any kind of random noise) which might be a good model for the underlying process, but rather on the possibility of recognizing a weaker form of determinism consistent with all possible tests.

Nonlinear analysis of series of natural phenomena therefore requires special attention: all available methods are needed in order to explore the phenomenon from every side. In fact after having done this, we may expect to find ourselves not in front of irrefutable proofs which demonstrate the presence of low-dimensional deterministic chaotic dynamics but, at best, with clues which do not enable its exclusion.

World Scientific Publishing Co. Pte. Ltd., Farrer
Road, Heuston Street, Covent Garden, London

For all other countries, including photocopying,
permission from the Copyright owner.
World Scientific, 222 Rosewood Drive, Danvers, MA

Published in January, April, July and October
Subscription rates available upon request

World Scientific Publishing Services,
200 Meacham Avenue, Elmont, NY

The present work is concerned with the analysis by nonlinear dynamical methods of the behavior of river flow. With regard to the component linked to the rainfall regime, the study contributes to the wide field of research on climate. On the other side, the system presents two further aspects which are also extremely relevant: that of the response of a river basin to precipitations, with its runoff mechanism formation; and that, concerning engineering, of flood forecasting.

Considering the climatic aspect, the approach to time series with nonlinear methods is not new: chaos theory methods have been applied to various natural phenomena of environmental interest, many of which were concerned precisely with climate dynamics. Due to the extension of the problem, the subtlety of the analyses in question, and the difficulty of obtaining sufficient reliable data, a lively scientific debate is currently going on (see Refs. 52, 57, 96 and the references therein). Further arguments related to climate dynamics have likewise been confronted in other works, with interest focused also on the engineering aspects of the problem.^{76,82}

Despite the aims and motivations partially in common with these latter studies, the phenomenon examined here has its own particular characteristics, which are to be added to the climatic component and make it a candidate for low-dimension nonlinear dynamics. While, in fact the debate on the presumed climate attractor is above all centered on the dialectics between the apparent excessive complexity of the system and its description in terms of low-dimension dynamics, in the case of riverflow the effect of the river network, the aquifers, glaciers and lakes can contribute (if the climate itself is not already of a low dimension) to a reduction of the complexity of the system. To suggest such a possibility is the fact that the flood formation mechanism is affected by the topology of the river network, strongly enough as to be better pictured in terms of fractal geometry (for example, Refs. 38, 63, 75 and the references therein), and by other characteristics like the geometry of the basin, the presence of storage capacities (lakes, glaciers or snowfields), the geology, etc. Some of these factors have in part been linked with the possible presence of chaotic dynamics^{1,98} regarding, respectively, the behavior of runoff due to snowmelt in a small mountain basin, and the discharges from sewer systems in large cities.

Besides the works cited, which are not directly concerned with the problem of riverflow, we are not aware of any studies which have investigated the presence of deterministic chaos in the discharge time series of a natural water course. Three articles^{41,42,44} are nevertheless to be noted which, without investigating the presence or the features of an underlying deterministic chaotic dynamics, have explored the possibility of forecasting discharges of a river using statistical methods in some way referable, even though only formally, to chaos theory.

It appears therefore useful to undertake a detailed examination of the possibility of the existence of deterministic chaos in the discharge time series of a river. Recognizing a low-dimensional chaotic dynamics would on one side enable us to improve flood-formation models, and on the other allow us to make forecasts which are more reliable on short-term, and thus important for civil protection.

The present work is concerned with the analysis by means of the component linked to the rainfall regime, the study contributes to the wide field of research on climate. On the other side, the system presents two further aspects which are also extremely relevant: that of the response of a river basin to precipitations, with its runoff mechanism formation; and that, concerning engineering, of flood forecasting.

Considering the climatic aspect, the approach to time series with nonlinear methods is not new: chaos theory methods have been applied to various natural phenomena of environmental interest, many of which were concerned precisely with climate dynamics. Due to the extension of the problem, the subtlety of the analyses in question, and the difficulty of obtaining sufficient reliable data, a lively scientific debate is currently going on (see Refs. 52, 57, 96 and the references therein). Further arguments related to climate dynamics have likewise been confronted in other works, with interest focused also on the engineering aspects of the problem.^{76,82}

2. General Features

The data used in this study are those of the Dora Baltea, orographic section. The series is taken from 1st January 1970 to 31st December 1998. The measured section is located in a region in northwestern Italy, with a surface area of 3313 km², of which 2080 m above sea level. The minimum, corresponding to the

Given the rainfall regime, the geometry of the basin, its topography and lakes, the river discharge is highly irregular. Besides, the presence of forests and urban areas make such a situation more complex, as discussed in the Introduction.

The discharge time series of the water course in the study area has been taken and calibrated using the geometrical area of the basin. The data can be affected by a number of significant errors and by errors in the measurement of the liquid section. On the occasion of large floods, the measure correctly of the liquid section may alter the measurements, which, in further elaborations, we will

The present work reports the results on the geometry of the conjectured attractor by means of the correlation integral and the dimensions linked to it, and analyzes the local dynamics through nonlinear prediction.

The paper is structured as follows: after a brief outline of the characteristics of the time series measured (Sec. 2), the results of the traditional statistical and spectral analyses are reported (Sec. 3). The subsequent part deals with the problem of the reconstruction of the attractor in phase space (Sec. 4). Section 5 reports the results on the correlation dimension, which are corroborated by some simple verifications presented in Sec. 6. Sections 7 and 8 deal with nonlinear prediction, seen above all as an instrument to investigate nonlinear dynamics. Section 9 summarizes the results obtained, drawing conclusions and perspectives.

2. General Features of the River Flow Series

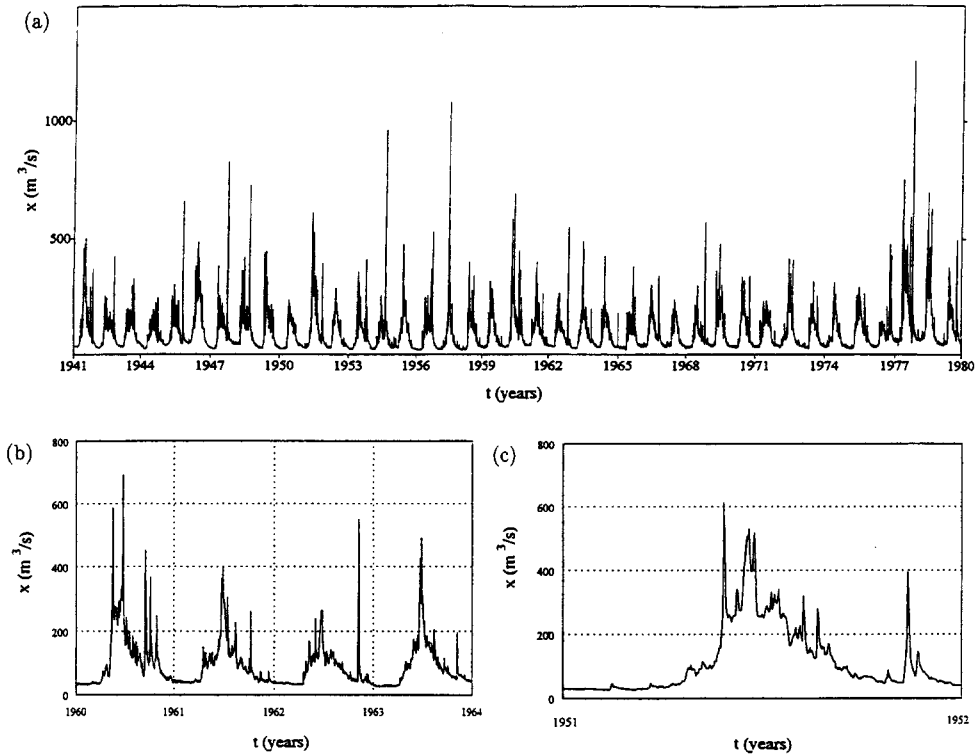
The data used in the present work is part of the series of mean daily discharges of the Dora Baltea, orographic left tributary of the river Po, measured at the Tavagnasco section. The series consists of 14246 measurements, taken uninterruptedly daily from 1st January 1941 until 31st December 1979 by the Po Hydrographic Office. The measured section subtends the entire river basin of the Aosta Valley, alpine region in northwest Italy. The predominantly impermeable basin has an extension of 3313 km², of which about 190 are glacial areas; the average height of the basin is 2080 m above sea level, the maximum 4807 m above sea level (Monte Bianco), and the minimum, corresponding to the section measured, 263 m above sea level.

Given the rainfall regime, the geographic position, the fairly considerable extension of the basin, its compact form, and the presence of numerous glaciers, snowfields and lakes, the river flow of the Dora Baltea is of the glaciopluvial kind, not very irregular. Besides, numerous large and small valleys and a wide area of pasture and forest make such a water course a valid representative for a first study of the kind discussed in the Introduction.

The discharge values are obtained by evaluating the free surface level of the water course in the measuring section, from which the rating curve of discharges is taken and calibrated. This links the discharges to the height of the water through the geometrical and hydraulic characteristics of the section of the water course. The data can be affected by a certain imprecision, reflected in the rather modest number of significant digits of the measurement (reported to one tenth of m³/s) and by errors in the valuation of the discharges. The latter are accentuated on the occasion of large flood discharges, both because it is then more difficult to measure correctly the levels reached from the free surface and the characteristics of the liquid section, and because erosions and deposits from extreme hydrological events may alter the characteristics of the section itself. To such disturbances to measurements, which should be taken carefully into consideration in the subsequent elaborations, we also need to add human activity factors, manifested in withdrawals

for hydroelectric use, irrigation, aqueducts, etc. For the Dora Baltea river, in the section under examination, such effects are fortunately relatively contained with respect to those observed in other water courses.

Figure 1a shows the discharge time series, some details of which have been enlarged (Figs. 1b-c). Clearly visible are the flood peaks and the seasonal periodicity, with both large and small discharges during the year.



Figs. 1a-c. Discharge time series behavior.

Table 1

mean	92.8 m^3/s
standard deviation	80.7 m^3/s
skewness	2.7
kurtosis	18.0
maximum	1260.0 m^3/s
minimum	18.0 m^3/s

Table 1 shows the function, which dis

3. Autocorrelation

The study of the first important characteristics were

In order to avoid to standardize the from its average

Representing the

$$x(t_0), x(t_0 +$$

with $N = 14246$, $0, \dots, N - 1$, the r

where the overline

The autocorrela

represents the self-enables us to pick u

Saltea river, in the
ly contained with

which have been en-
seasonal periodicity,

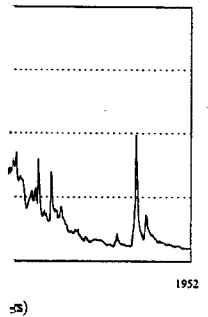
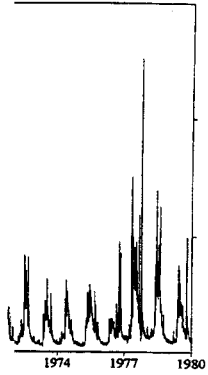


Table 1 shows the principal data of the series; Fig. 2 shows its probability density function, which displays an exponential behavior for high discharge values.

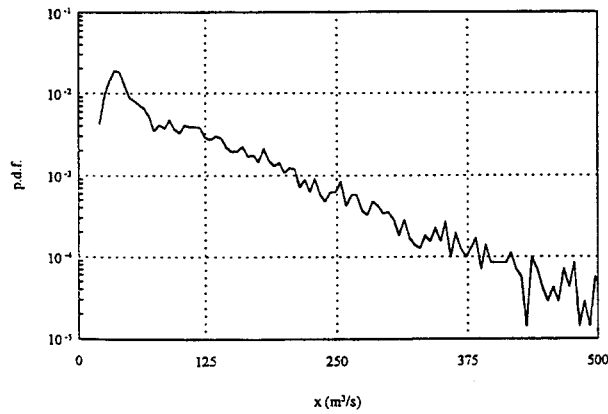


Fig. 2. Probability density function.

3. Autocorrelation and Power Spectrum

The study of the autocorrelation and the spectral analysis should provide^{4,14,69} the first important indications on the aperiodicity of the time series whose principal characteristics were outlined in Sec. 2.

In order to avoid distortions in the spectrum and autocorrelation estimates, and to standardize the results, we use a normalized, dimensionless signal, subtracting from it its average and dividing the resulting series by its standard deviation.

Representing the equispaced discharge series as

$$x(t_0), x(t_0 + \Delta t), x(t_0 + 2\Delta t), \dots, x(t_0 + i\Delta t), \dots, x(t_0 + (N - 1)\Delta t) \quad (1)$$

with $N = 14246$, and writing the i th value as $x_i = x(t_i)$, $t_i = t_0 + i\Delta t$, $i = 0, \dots, N - 1$, the new normalized dimensionless series is

$$\xi_i = \frac{x_i - \bar{x}}{\sqrt{\overline{(x_i - \bar{x})^2}}}, \quad (2)$$

where the overline represents the time average, $\bar{x} = \frac{1}{N} \sum_{i=0}^{N-1} x_i$.

The autocorrelation, defined as

$$\rho(\tau) = \overline{\xi(\tau)\xi(t + \tau)}, \quad (3)$$

represents the self-correlation of the signal for different values of time lag τ and enables us to pick up possible linear links between values at different times.

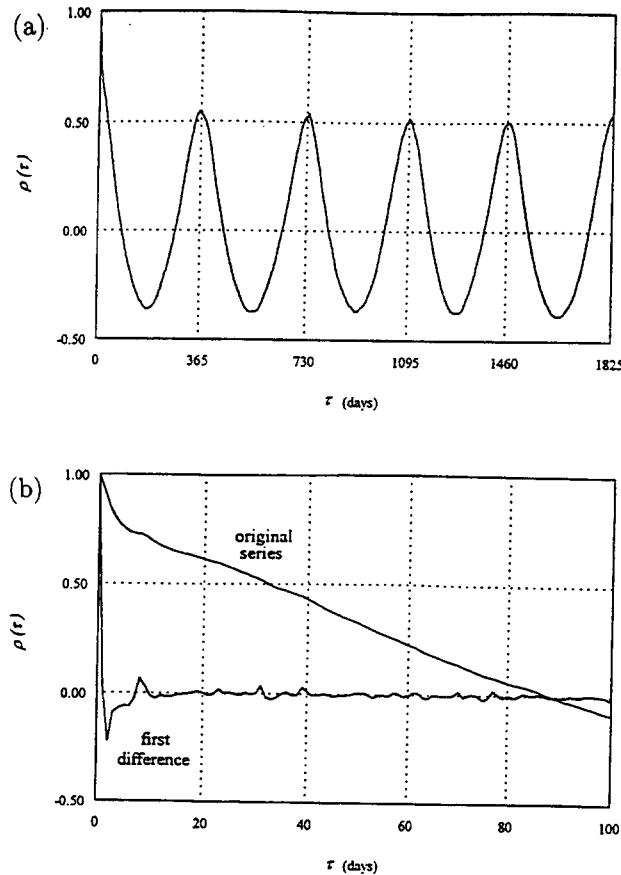


Fig. 3. (a) Autocorrelation of the original series. (b) Detail of the autocorrelation of the original series and that of the first difference series.

Figure 3 shows the autocorrelation for values of τ ranging between 0 days to about 5 years. After a rapid decrease of the autocorrelation, which takes place in 7–10 days, the function shows a regular behavior, which represents the effect of the seasonal character of the discharges, due, besides rainfall regime, to the presence of numerous glaciers and snowfields which “breathe” with the seasons. It is important to underline the initial abrupt fall of the autocorrelation, visible in detail in Fig. 3b. This indicates a complex behavior, characterized by a time scale of a few days, and grafted onto the general behavior which is certainly not periodic yet has seasonal characteristics over annual frequency. The autocorrelation of the first difference signal, $(x_i - x_{i-1})$, in Fig. 3b, shows a rapid monotonic decrease in autocorrelation. This fact will be used later to investigate the effects of correlation of the original signal.

The character of complex aperiodicity and irregularity is even more apparent when one looks at the frequencies. The power spectrum in fact shows the degree

to which the v
the signal.

The express

so that $\int_0^{+\infty} S$
Hanning windo
finally averagin

Figures 4a–
peak at a frequ

to which the various harmonics present combine to form the whole variance of the signal.

The expression used for the power spectrum is

$$S(f) = 2 \int_{-\infty}^{+\infty} \rho(\tau) e^{-i2\pi f\tau} d\tau, \quad (4)$$

so that $\int_0^{+\infty} S(f)df = 1$. The spectrum was calculated by applying the usual Hanning window, then using the FFT algorithm on blocks of 4096 values, and finally averaging out the spectra obtained.

Figures 4a-b show the behavior of the power spectrum. In evidence is the peak at a frequency of about $1/365 \text{ days}^{-1}$, due to the seasonal component, and

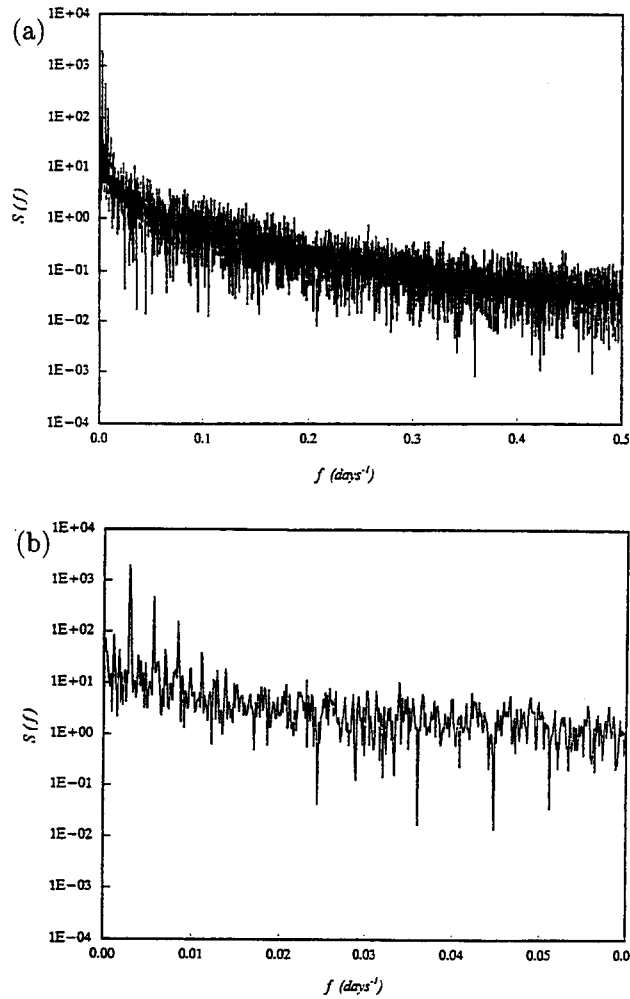


Fig. 4. (a) Power spectrum. (b) Detail.

ation of the original

etween 0 days to
ch takes place in
s the effect of the
o the presence of
s. It is important
detail in Fig. 3b.
f a few days, and
yet has seasonal
e first difference
autocorrelation.
a of the original

more apparent
ows the degree

accompanied by correspondingly higher harmonics. The fact that the spectrum is continuous with a pronounced and wide base shows clearly the aperiodicity of the series.

4. Reconstruction of the Attractor

The irregularity of the series could be due as much to a low-dimensional deterministic chaotic dynamics, as to the action of a very large number of variables, or even to a combination of the two.

The first step in the search for possible traces of a deterministic behavior is that of attempting to reconstruct the dynamics in phase space. Having available the time series of only one of the variables present in the phenomenon, namely the discharge x_i , we can use the delay-time method due to Takens⁸⁶ (see also Ref. 61), based on the conjecture that the interaction between the variables is such that each component contains information on the complex dynamics of the system. Choosing a delay time τ (usually a multiple of Δt), the method entails the construction of a set of $[N - (m - 1)\tau/\Delta t]$ vectors, of dimension m , of the form

$$\mathbf{x}(t_i) = \{x(t_i), x(t_i - \tau), \dots, x(t_i - (m - 1)\tau)\}, \quad (5)$$

where m ($m = 2, 3, \dots$) is called the embedding dimension. In the m -dimensional space such vectors describe, over time, an object topologically equivalent to the attractor of the physical system from which x was measured provided that such an attractor exists, if $m \geq 2D + 1$, where D is the fractal dimension of the attractor. Apart from the latter conditions on the value of m , in theory there should not be any other limits to the choice of the parameters m and τ . However in practice, as Takens' theorem presupposes series of infinite length and completely void of errors of measurement, practical application of the method proves of course heuristic.

As for the choice of m , D not being known *a priori*, various methods have been proposed (see Ref. 34 and the references therein). In order to implement operationally the above conditions, increasing values of m are used, compatible with the practical limitations imposed by the number of points available; then the various quantities are estimated, and one checks whether above a certain value, say m^* , they remain almost constant. One then adopts $(2m^* + 1)$, as correct embedding dimension.

More controversial and complex is the choice of the value of τ . No preferred criteria exist so far.^{8,12,34} What is certain is that values which are too low give coordinates which are excessively correlated in time (a phenomenon called redundancy), whilst $x(t_i)$ and $x(t_i - (m - 1)\tau)$ no longer have a connection if τ is too large (irrelevancy). Within these limits, the most appropriate estimate of the value for τ is made by comparing the results of various methods and eventually taking the smallest. Some criteria propose using the autocorrelation (for example, Refs. 82, 94 and 74), adopting as τ the time at which the autocorrelation first reaches a certain conventional value. Others instead suggest choosing a value equal to a fraction of

the dominant period ($T/4$). Finally, more its generalization by those, more recent, considerations for a some experimental in ing various values of on the actual value of

Regarding the se and on dominant pe 30 days and 90–100 the presence of a se producing a link wh belonging to a certai periods of the order almost independent; large. Similarly, as t hourly variations, th be considered oversa would be better cho

In support of su recent methods prop maximum spreading

In the fill-factor Refs. 7 and 8), the op of the fill-factor func dimensional parallel principal advantages particular robustnes when the attractor h the Lorenz attractor into account the loca

Figure 5a shows t culation of the funct with equal probabilit

It can be seen hov the attractor correspo for τ equal to 4 and seasonal nature of th of the diagram (Fig. as to a possible choic they show some sli for $m = 9-10$. This

the dominant periodicity T (for example, Ref. 96 proposes T/m ; whilst Ref. 19 uses $T/4$). Finally, more complex approaches, such as that of Frazer and Swinney²⁷ and its generalization by Liebert and Schuster,⁴⁸ are based on mutual information, or those, more recent, (Refs. 7, 8, 9 and 49) which propose topological or geometrical considerations for a correct reconstruction of the attractor. Despite this criteria, in some experimental investigations the problem has been solved more simply considering various values of τ and proving that the results do not show a strong dependence on the actual value chosen.

Regarding the series under examination, the criteria based on autocorrelation and on dominant periodicity (Figs. 3a-b and 4a-b) would give a value of τ between 30 days and 90-100 days. Such a choice, however, would be misleading, because the presence of a seasonal component increases the autocorrelation of the signal, producing a link which does not correspond to a dynamic connection between data belonging to a certain flood event. In fact, leaving aside the seasonal component, for periods of the order of a month the discharge values can be considered dynamically almost independent; so that we are already beyond the limit for which τ is too large. Similarly, as the behavior of the discharge of a water course can present even hourly variations, the discharge series available, made up of daily averages, cannot be considered oversampled. So, at least intuitively, a reliable value of the delay time would be better chosen of no more than a few days.

In support of such a suggestion, it appears useful to apply two of the most recent methods proposed; the fill-factor method and the criteria which ensures the maximum spreading of trajectories.

In the fill-factor method, proposed by Buzug, Reimers and Pfister⁹ (see also Refs. 7 and 8), the optimum τ is chosen as that corresponding to the first maximum of the fill-factor function, defined as the logarithm of the average volume of all m -dimensional parallelepipeds, defined by the points of the attractor. Among the principal advantages of this method are the relative rapidity of elaboration and the particular robustness with respect to the effects of noise. However, in some cases, when the attractor has more than one unstable focus (this happens, for example, for the Lorenz attractor), this method does not provide useful indications not taking into account the local properties of the attractor.

Figure 5a shows the behavior of the fill factor for the discharge series. In the calculation of the function, a number of reference points were used, chosen at random with equal probability, equivalent to 5% of the total number of points.

It can be seen how, for values of τ between 10 and 20 days, the reconstruction of the attractor corresponds almost to the maximum use of phase space. Beyond this, for τ equal to 4 and 6 months, the fill factor exhibits relative minima due to the seasonal nature of the phenomenon. Looking at the enlargement of the first part of the diagram (Fig. 5b), we see that the various curves do not provide indications as to a possible choice of τ up to embedding values of 4-5, whilst for higher values they show some slightly pronounced maxima at $\tau = 3$ for $m = 6-8$, and $\tau = 2$ for $m = 9-10$. This not only confirms that the optimum delay-time value must be

distance r , and $C_m(\tau, r)$ is the correlation integral

$$C_m = \frac{1}{M^2} \sum_{i \neq j}^M \vartheta(r - \|\mathbf{x}_i - \mathbf{x}_j\|), \tag{7}$$

where ϑ is the Heaviside step function, $\|\cdot\|$ indicates a norm of the vector, and M is the number of points of the reconstructed attractor. The optimum τ is obtained when $P_m(\tau, r)$ presents its first relative minimum, that is when, on average, changing the embedding dimension from m to $m + 1$, a point undergoes the minimum reduction of its neighbors. Beyond this, for values of m greater than the first sufficient to correctly embed the attractor (i.e. when the addition of a further coordinate does not provide any more information), the graph of $P_m(\tau, r)$ versus τ loses significant minima and converges towards an accumulation line. From the slope of this curve for very small values of τ it is also possible to estimate the K_2 entropy.⁸ Considering that the correlation integral is itself a measure of mutual (Renyi-)information,³⁴ the method is similar to that presented by Liebert and Schuster,⁴⁸ which considers the mutual information between m -dimensional coordinates obtained with Takens' technique.

Contrary to what is proposed by the authors of the method, the calculation in the present implementation is extended to all the points of the series, without limitations: this expedient, made possible by the use of the box assisted algorithm for a rapid search of the neighbors (which will be described in Sec. 6), provides a better convergence of the mean values for high embedding dimensions and small values of r .

The result of our calculation of $P_m(\tau, r)$, for values of τ between 1 and 200 and m between 2 and 10, is shown in Fig. 6a; Fig. 6b shows an enlargement of the initial part. The value of r used corresponds to the zone in which there appears to exist a certain convergence of the correlation dimension (see Sec. 6).

For values of τ greater than 10–12 days the curves begin to present pronounced oscillations, which develop along an average, essentially flat behavior, which belongs to values of τ for which there is no longer any connection with the data. Clearly visible is the common increase at 4 months and 6 months, corresponding with what we observed in the behavior of the fill factor. Below $\tau = 10$ –12, the curves show, at the increase of m , a pronounced convergence on a line with an evident negative slope. The irregular behavior which the curves present relative to higher values of m is due to the lack of a sufficient number of points in correspondence with those τ for which the attractor is more dispersed. Globally, up to seasonal fluctuations, the behavior is analogous to that obtained applying the same method to the Hénon map: in this case the appropriate delay time is that provided by the map itself, and the curves which represent $P_m(\tau, r)$, after a linear decrease, are horizontal for values of τ at which the data no longer shows dynamical correlations. The periodical presence of common maxima on various curves (7, 14, 21, ... days) should also be noted, which we are at present unable to explain. Analogous periodic behavior is found in the redundancies of the Rössler attractor.^{62,67}

(6)

ue of m to adopt
 r than 4–5, since
 icular structures,
 rity that denotes
 ed by Buzug and
 ion should ensure
 following function
 ries:
 n average within



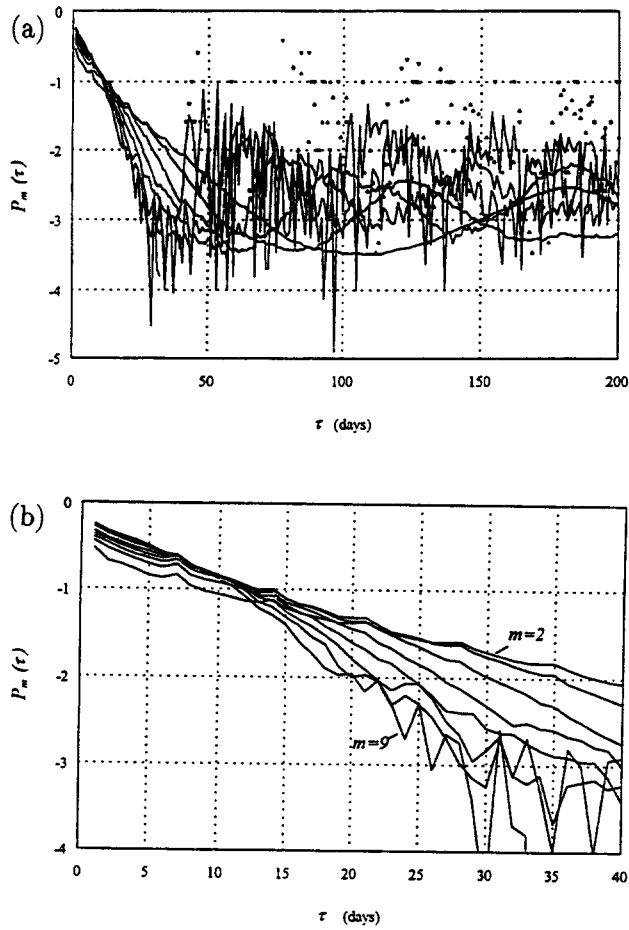
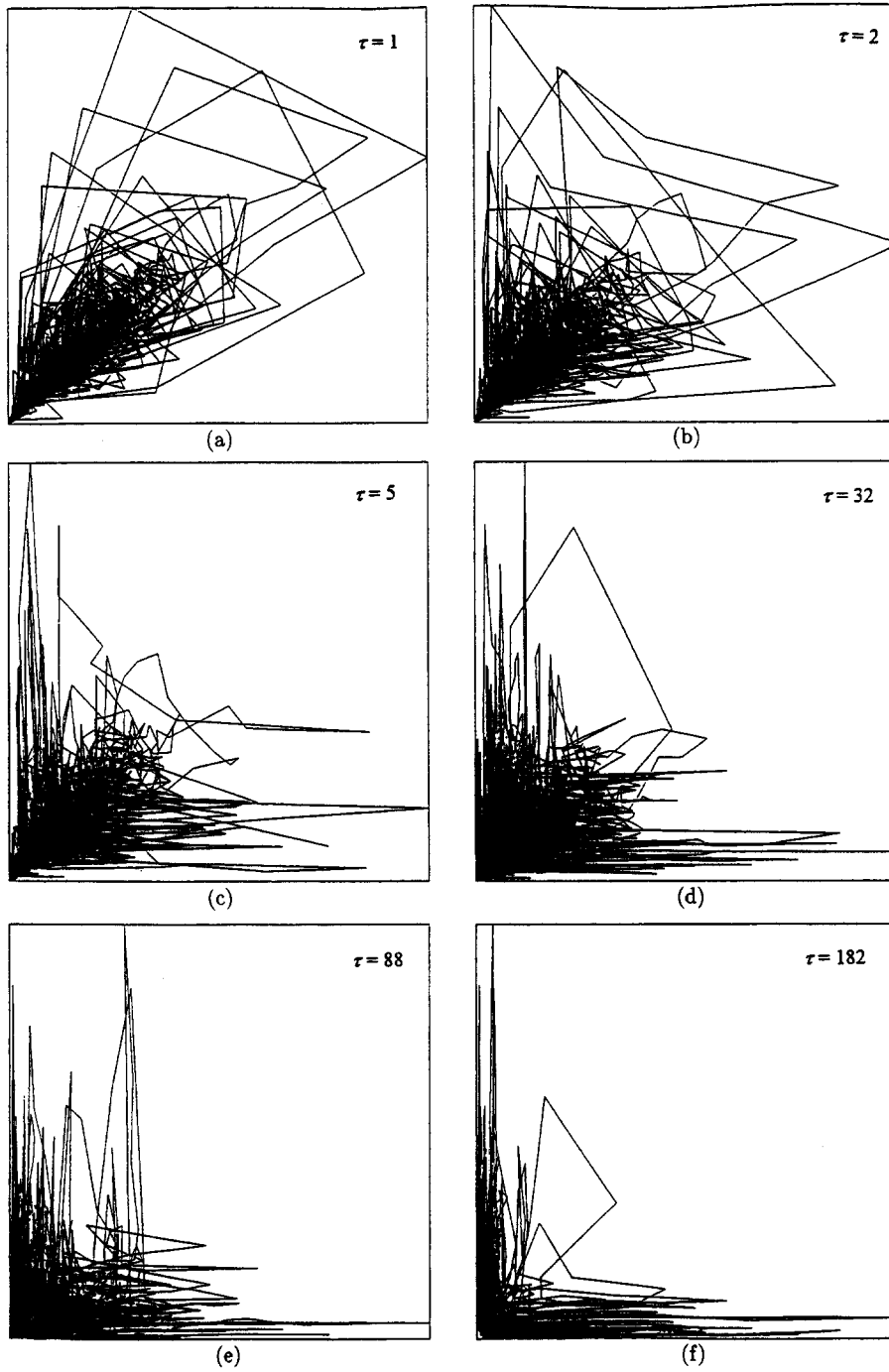


Fig. 6. (a) Maximum spreading of trajectories: $P_m(\tau)$ behavior (the isolated symbols represent the values of $P_m(\tau)$ for $m = 8$ and 9 where it was possible to calculate only a few points). (b) Detail.

Figure 6b shows in greater detail the various curves of the initial zone. In the section where they converge on a line, these do not exhibit pronounced minima (very minor ones might perhaps exist at the values 2, 5, 6 days) and therefore cannot provide more precise indications, consistent with the measurement resolution, for the choice of τ , beyond the fact that it must not have a value larger than around 10–12 days. For higher values the line of convergence begins to disappear and the dynamical structure of the attractor is lost: this is in accord with what the fill factor showed and is in agreement as well with results from the application of nonlinear prediction. With regard to the embedding dimension, we observe that passing from 4 to 5 it practically reaches complete convergence on a line: once more the result corresponds to that of the fill factor.



Figs. 7a–f. Projected delay times.



Figs. 7a-f. Projections of the reconstructed attractors on the plane $x(t) - x(t + \tau)$ with different delay times.

symbols represent
by a few points).

itial zone. In
anced minima
erefore cannot
resolution, for
r than around
ppear and the
t the fill factor
n of nonlinear
t passing from
ore the result

The considerations made up to now suggest very low values of τ . A verification of a purely visual kind may make such a conclusion more evident: Figs. 7a–f show on the plane $x(t) - x(t + \tau)$ the projections of the reconstructed attractors for values of τ of 1, 2, 5, 32 (1 month), and 182 days (6 months) respectively.

Even though the projection for $\tau = 1$ day presents a certain thickening on the first bisectrix (corresponding to the periods during which the discharge has no considerable variation), for the other periods the dynamics appears to be well represented. On the contrary, when τ is greater than 2–3 days, this typical structure gradually disappears. For values greater than 7–10 days the various projections are practically indistinguishable. For all these reasons, and on the basis of what was obtained from the fill-factor method and the maximum spreading of trajectories, values of $\tau = 1$ and $\tau = 2$ will be used in what follows. Occasionally checks will be made with different values of τ .

We note that the shape of the projection of the reconstructed attractor with $\tau = 1$ and $\tau = 2$ resembles that of other physical systems in which evidence of chaotic dynamics has been recognized, for example, the Rössler attractor and those of velocity series measured in weak turbulence of Taylor–Couette.^{5,23} Even closer is the resemblance to the attractor reconstructed from the time series of sunspots.⁵⁵ With regard to the latter phenomenon we note that also the time series and the power spectrum are quite similar.

5. Correlation Dimension

Systems in equilibrium characterized by chaotic dynamics move on strange attractors, associated with at least one positive Lyapunov exponent, with fractal dimension D . Having previously reconstructed the attractor, the present section proceeds to the estimate of its fractal dimension, to which the number of excited modes in the system is linked (or, equivalently, the number of variables necessary to characterize the dynamics).

In general, the evaluation of D does not follow directly from its definition but through the calculation of the correlation dimension, according to the method proposed by Grassberger and Procaccia.^{32,33} If the phenomenon is chaotic and the attractor is correctly reconstructed, for a sufficiently large number of points and very small values of r , beyond a certain m the correlation integral follows the power law

$$C_m(r) \propto r^v, \quad (8)$$

where v is the correlation dimension, which provides a (generally good) estimate for defect of the fractal dimension D of the attractor.

We begin with a few comments on the method of calculation utilized.

First of all, the so-called infinite norm has been adopted in place of the Euclidean one, because it provides a lower computational burden and leads to more reliable results. Secondly, the use of the box assisted algorithm for the fast search of neighbors, proposed by Theiler⁸⁸ and implemented according to the optimization

elaborated by G...
ing it easier to re...
to the maximum

Among the c...
effect of the at...
berg and Essex⁵...
autocorrelation...
nounced knee be...
ignoring the effe...
second effect, wh...
carefully account...
the exclusion of

Tests carried ou...
for the discharg...
distorted by aut...
discard the mos...
in the calculatio

The problem...
From the most...
the correlation...
deductions up...
analysis to larg...
shall show happ...
not continue to...
of m before this...
of the significan...
and their releva...
always giving t...
the precautions...
short time serie

The behavio...
with $\tau = 1$ day...
deviation and r...
mentioned satu...
the behavior ap...
the effects due...
precision of the

In order to...
and of saturatio

elaborated by Grassberger,³¹ allows us a drastic reduction in calculation time, making it easier to realize numerous tests and to resort, as described in the last section, to the maximum spreading of trajectories method.

Among the causes which can produce distortions in the estimate of v are the effect of the attractor boundary, which was studied for white noise by Neremberg and Essex⁵⁶ and produces a weak underestimation, and the effect of the time autocorrelation between successive data in the attractor, which can produce a pronounced knee bend in the behavior of the correlation integral.^{81,87} We expect that ignoring the effect of the boundaries should not sensibly affect results. As for the second effect, which can in some cases completely distort the evaluation of v , it was carefully accounted for in terms of the following modified formula,⁸⁷ which enables the exclusion of temporally correlated points

$$C_m(r) = \frac{1}{M(M-1)} \sum_{n=W}^N \sum_{i=1}^{N-m} \vartheta(r - \|\mathbf{x}_i - \mathbf{x}_j\|) . \quad (9)$$

Tests carried out with values of W up to and beyond 50 lead to the conclusion that, for the discharge data under examination, the correlation integral is practically not distorted by autocorrelations. It was however decided to adopt $W = 5$, in order to discard the most temporally correlated data, without reducing the amount of data in the calculation.

The problem of the minimum length of the series is in fact also very important. From the most recent indications (see Refs. 34, 93 and 96) on the convergence of the correlation integral, we see that the number of points available allows correct deductions up to embedding dimensions equal to 5–6. One can even push the analysis to larger values, at least if looking for qualitative indication only, if, as we shall show happens in the present case, the slope of the correlation integral does not continue to increase linearly but tends to reduce its growth with the increase of m before this reaches values which are too large. By way of further verification of the significance of the amount of data, the behavior of the correlation integrals and their relevant slopes were evaluated for samples with different amounts of data, always giving the same results. Such evidence has led us to omit the adoption of the precautions usually necessary for the estimate of the correlation dimension from short time series.^{36,39,65}

The behavior of the correlation integral (Fig. 8) for the reconstructed attractor with $\tau = 1$ day is fairly regular. For high values of r/σ , where σ is the standard deviation and represents a measure of the extension of the attractor, we get the mentioned saturation zone, whilst for small values we observe an interval where the behavior appears to be linear. Finally, for even lower values of r , we notice the effects due to the limited number of points (depopulation) and to the modest precision of the measurements.

In order to reach better indications on the possible presence of a scaling region and of saturation with the increase of m , Fig. 9 shows the slopes of the curves $C_m(r)$.

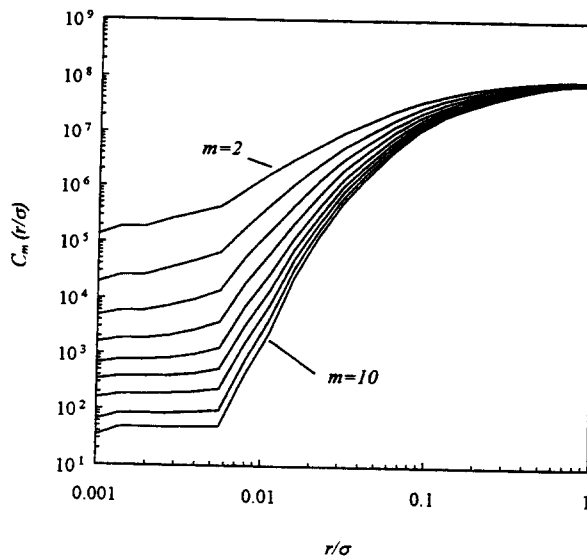


Fig. 8. Correlation integral behavior for m between 2 and 10 ($\tau = 1, W = 5$).

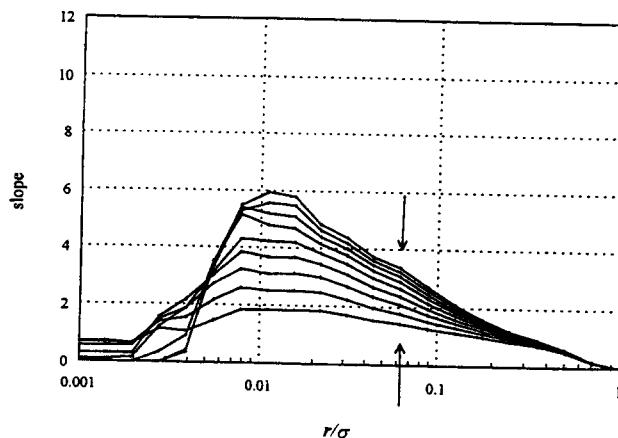


Fig. 9. Correlation integral slopes for m between 2 and 10.

The values shown are calculated from the data of the previous figure with three-point formulas (the slope calculated on two points, even though slightly more irregular, shows an analogous behavior).

The behavior of the slopes is interesting: between the saturation on the right and the effect of noise on the left, we have an interval in which the curve is closest to the horizontal, with values less than 4. The pronounced growth of the slope for low values of r is typical of experimental series affected by errors and imprecisions of measurements, and to such factors the growth seems to be attributable (for white noise we have in fact $C_m(r) \propto r^m$).

To evaluate values of the to the horizon in relation to

slope

Fig. 10. Cor

Even though tion, such a l dimensional c tainly an inte

On the ot and even if it sufficient con happen that p make the cor correlated sto different dyn to have furthe to reduce the There were a considerable for example,

In conclus of the correla to the result trajectories.

To evaluate the degree of saturation and convergence at a particular value, the values of the slopes are shown (Fig. 10) for the section where the behavior is closest to the horizontal (corresponding to the values of r indicated by the arrows in Fig. 9), in relation to the embedding dimension.

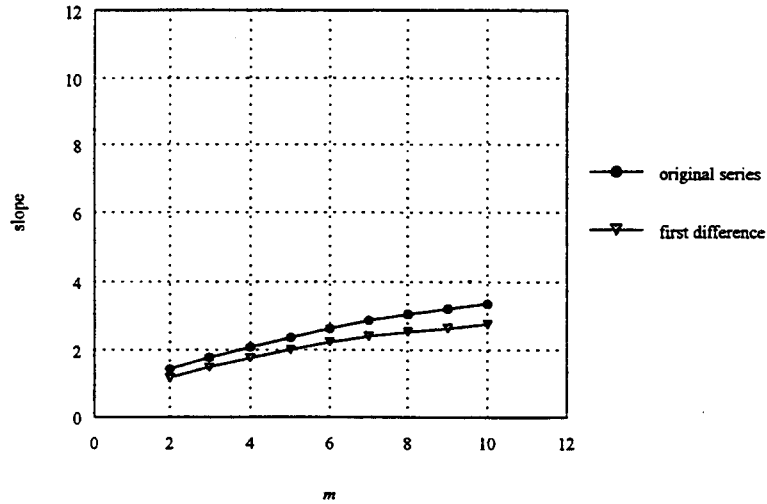


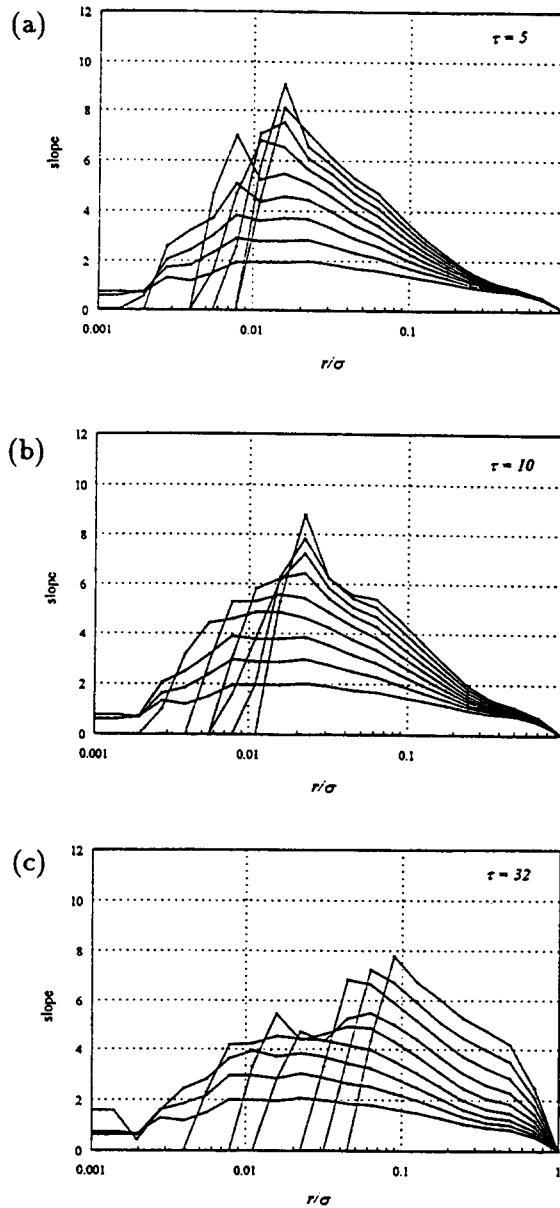
Fig. 10. Correlation integral slopes in the inflection zone versus the embedding dimension.

Even though a real plateau does not exist and there is no complete saturation, such a behavior of the correlation integral allows the possibility that a low-dimensional dynamics component might be present in the phenomenon. It is certainly an interesting fact that the value of $C_m(r)$ is always below 4.

On the other hand, the interval where the slope is constant is not very large, and even if it were better pronounced, it would only provide a necessary and not sufficient condition for proving the presence of a chaotic dynamics. It could also happen that possible underlying trends and other forms of correlation between data make the correlation integral look like that of a chaotic series, being in reality a correlated stochastic series.^{60,72,89} Even a strong intermittency or the presence of different dynamics simultaneously active can give rise to wrong results.³⁴ In order to have further indications we need then to subject the series to verifications and try to reduce the effects of instrumental disturbance, using noise reduction techniques. There were actually cases in which the application of these techniques brought in a considerable improvement in the convergence of the correlation integral slopes (see for example, Ref. 79, Figs. 1 and 3).

In conclusion of this section, we note that the reduction in growth of the values of the correlation integral slope from values of $m > 4-5$ corresponds substantially to the results obtained from both the fill factor and the maximum spreading of trajectories. Also, the behavior of the correlation integral and its relevant slopes

calculated on the reconstructed attractor with different values of τ (Figs. 11a-c) confirms our previous observations about the choice of τ . Apart from the lowest values of delay time, the dynamical link between data is lost early and the curves of the slopes grow analogously to how they would do in the presence of a white noise.



Figs. 11a-c. Correlation integral slopes for different values of τ ($W = 5$).

6. Some S

The effect, correlation, chaoticity f

The first to the first governed b signal and between th strong stoc to disturba by the ope



(b)



Figs. 12a-c. constructed wit

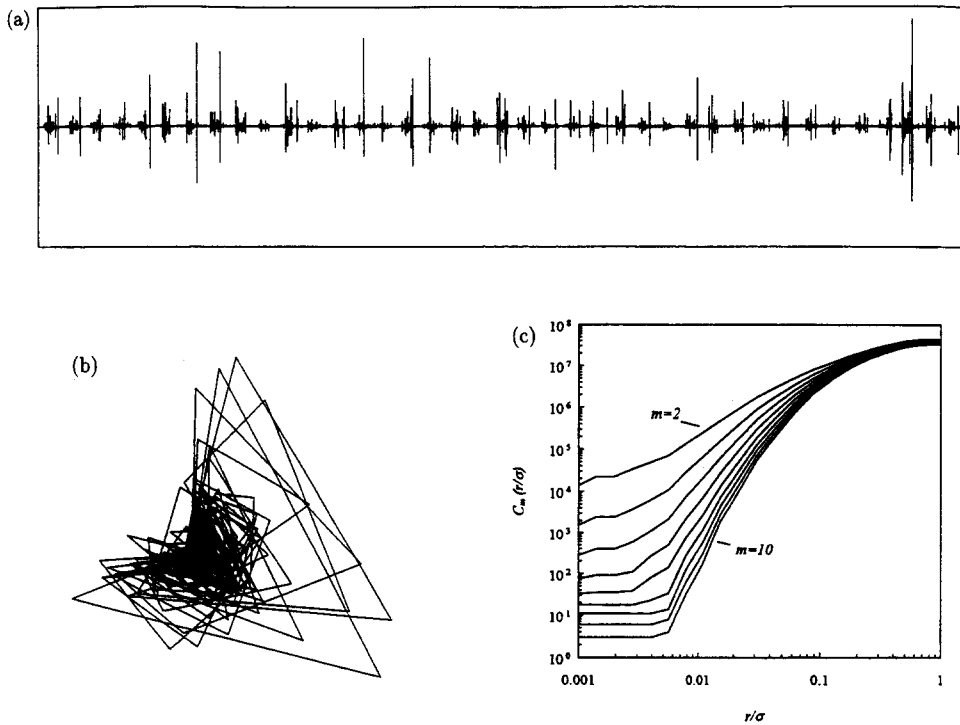
Figure the projec the latter, see that the original sig

values of τ (Figs. 11a-c). Apart from the low- τ case, the correlation integral is lost early and the results do in the presence of a

6. Some Simple Tests

The effect, mentioned above, of a possible non-stationarity of the series on the correlation integral has stimulated the preparation of various tests to distinguish chaoticity from randomness.

The first consists in comparing the results of the original series with those relative to the first difference series ($x_i - x_{i-1}$). As Provenzale *et al.*⁷³ observed, for a system governed by a low-dimension strange attractor, v is the same for both the original signal and that of its first differences, so that the observation of a marked difference between the values of the two series could be a good indication that the signal has a strong stochastic component. Against the simplicity of the method is its sensibility to disturbances, which may reduce its sensitivity and moreover could be amplified by the operation of difference performed on the signal.



Figs. 12a-c. First difference signal. (a) Complete series. (b) Projection of the attractor reconstructed with $\tau = 1$ day. (c) Correlation integral behavior ($\tau = 1$, $W = 5$).

Figures 12a and b show, respectively, a section of the first difference signal and the projection of the corresponding reconstructed attractor using $\tau = 1$ day. In the latter, as well as in the behavior of the correlation integral (Figs. 12c-d), we see that the difference series preserves the imprint of the dynamics present in the original signal.

of τ ($W = 5$).

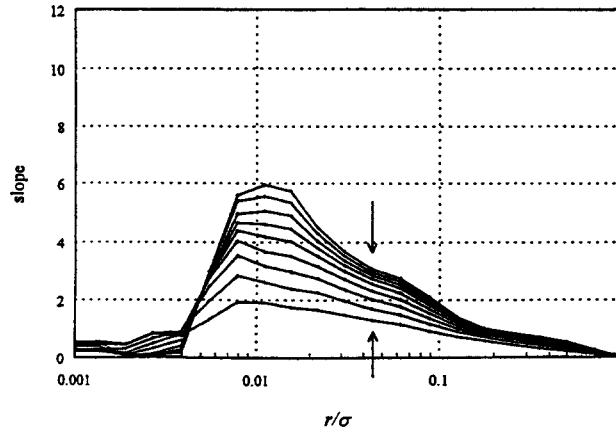


Fig. 12d. Difference signal: $C_m(r)$ slopes for m between 2 and 10.

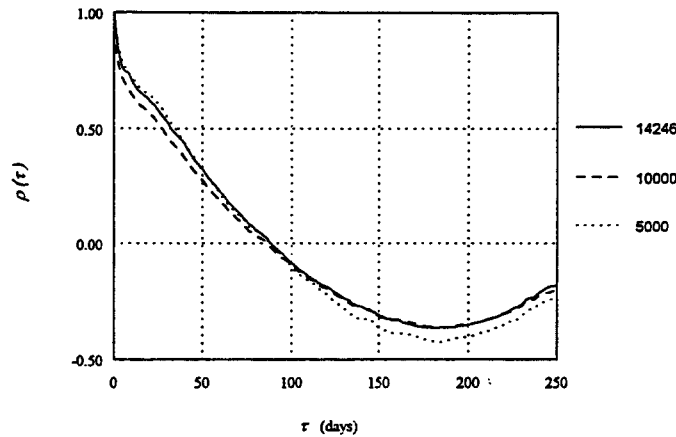


Fig. 13. Comparison of the discharge series autocorrelations calculated with differing numbers of points.

In order to make the comparison more concrete, Fig. 10 shows, on the same graph, the correlation integral slopes versus m , for both the discharge and difference series: the test appears to confirm the presence of a low-dimensional deterministic dynamics.

The second test considers the dependence of the autocorrelation on the lengths of the series from which it is derived: as noted by Tsonis, Triantafyllou and Elsner,⁹⁶ if the time in which the autocorrelation goes to zero does not continue to grow with the number of points considered, then it may be assumed that the series is not a fractal Brownian motion and that the process is stationary. Figure 13 shows the behavior of the autocorrelation calculated with the first 5000, the first 10000,

and with all the points up to the oscillation considered possible. The series may be

7. Nonlinear

We may conclude that the presence of a low-dimensional deterministic dynamics is therefore with

Since its value. On the other hand, the fact^{11,25,31} that those obtained with ARMA, ARMA, ARMA present in the

On the other hand, the importance of the result of the reliability, such as only mimic series

We shall consider the possibility of making forecasts of dynamics which, though it may be the same time — forecasts. Obviously, understood in the local Lyapunov

Several authors have made forecasts and Sidorowich's prediction. In this case, whether a chaotic

Practically, starting from the (Sec. 4) in physics, the form of a

where $x(t)$ is a system at time t , a good approximation

and with all the available points, respectively. All behaviors are essentially identical, up to the oscillations due to the number of points: thus even this check may be considered positive, and allows us to exclude the possibility that the irregularity of the series may be due essentially to the presence of correlated stochastic noise.

7. Nonlinear Prediction

We may conclude, from the analysis of previous sections that clues exist indicating the presence of a chaotic dynamics in the phenomenon under study. We proceed therefore with the application of nonlinear prediction to the time series.

Since its formulation nonlinear prediction has actually always had a double value. On the one hand we may only consider its predictive aspect, focusing on the fact^{11,25,34,93} that within chaotic phenomena it allows better forecasts than those obtained with other traditional methods (for example, autoregressive models, ARMA, ARMAX, etc.), thanks to its capacity to pinpoint the nonlinear aspects present in the dynamics.

On the other hand, one may instead consider nonlinear prediction as one of the important indicators necessary to understand whether or not a time series is the result of a chaotic dynamics. Moreover, it allows us to distinguish, with good reliability, such a dynamics from others possibly present in the time series which only mimic some characteristic property of the chaotic series.^{21,22,71,85,93,95,96,97}

We shall concentrate mostly on the second of the above aspects. The possibility of making forecasts out of a time series is certainly connected with the type of dynamics which generates it. In particular the existence of a chaotic dynamics, though it may reduce the possibility to make long-term forecasts, would at the same time — in view of its deterministic character — allow us to make short-term forecasts. Obviously the expressions “short-term” and “long-term” should not be understood in an absolute way, but in relation to the value of the largest among the local Lyapunov exponents.

Several authors^{10,24,25,93,96,97} have gone as far as suggesting that the capacity to make forecasts is connected with the very existence of deterministic chaos. Farmer and Sidorowich,²⁵ in particular, speak about the autoconsistency of nonlinear prediction. In this sense, the results of nonlinear prediction can help to understand whether a chaotic dynamics is present in the phenomenon.

Practically speaking, the basic idea of nonlinear prediction is the following: starting from the time series available, once the attractor has been correctly constructed (Sec. 4) in phase space, of dimension m , it is possible to interpret the dynamics in the form of an m -dimensional map f_T

$$\mathbf{x}(t + T) = f_T(\mathbf{x}(t)), \tag{10}$$

where $\mathbf{x}(t)$ and $\mathbf{x}(t + T)$ are vectors of dimension m , describing the state of the system at times t and $(t + T)$, respectively. If, thanks to the available data sample, a good approximation \hat{f}_T , necessarily nonlinear, of f_T , can be built, an estimate



Figure 2 and 10.

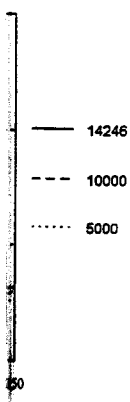


Figure 10 shows, on the same discharge and difference dimensional deterministic

relation on the lengths of Antafyllou and Elsner,⁹⁶ not continue to grow named that the series is binary. Figure 13 shows 5000, the first 10000,

$\mathbf{x}(t+T)$ of future values of $\mathbf{x}(t > t_{\text{fin}}$, the final time accounted for by the series) can then be obtained through the map

$$\mathbf{x}(t+T) = \hat{f}_T(\mathbf{x}(t)). \quad (11)$$

Of course there exists an infinite number of potential nonlinear models for \hat{f}_T and if no indications are given by the physics of the phenomenon considered, there is no single method to find the most appropriate shape of \hat{f}_T (except possibly, generalization criteria¹¹). Any choice has some degree of arbitrariness, therefore, the choice of the form of \hat{f}_T should be linked essentially to the complexity of the dynamics, to the extension as well as to the quality of the reference sample, and to the computational burden (both in terms of time and required memory).

Two different approaches to identify an optimal form for \hat{f}_T have been proposed, one global and the other local.

The first one tries to approximate the map (10) by working globally on the entire attractor, and searching for a map \hat{f}_T valid for any of its points. Examples of such an approach are: polynomial and rational functions (for example, Refs. 16, 24 and 93), radial basis functions,^{10,37,43} neural networks,^{3,18,21,28,47,58} and mixed methods.^{11,83}

The alternative method, which we follow here, is based instead on local approximations.^{16,24,25,30,50} It entails the subdivision of the \hat{f}_T domain into many subsets, each of which identifies some approximations \hat{f}_T , valid only in that same subset. In this way the dynamics of the system is described step by step, locally in phase space. This choice leads to a considerable reduction in the complexity of the representation \hat{f}_T , whilst avoiding to lower the quality of the forecast $\mathbf{x}(t+T)$. Some examples in the literature^{11,18,93} indicate that on very short time (up to values of T of the order of $4 \div 6\Delta t$, where Δt is the sampling time interval of the series), particularly when one has long reference series and the dynamics is not simple, the results obtained are generally better than those one gets with global methods. *Vice versa* for longer forecast times, due to the capacity of the latter methods to catch the global structure of the attractor.

The identification of the sets in which to subdivide the domain can be done in different ways. Disjoint sets may be considered¹⁶; however, in such a case problems can emerge at the boundary zones.²⁵ This can be corrected either by enforcing conditions of continuity at the boundaries of the subset, which can be difficult because of the phase-space dimension, or by allowing an overlap between adjacent subdomains.²⁵ The latter approach, which has become the most commonly used, entails first of all fixing a metric $\|\cdot\|$, then, given the starting point $\mathbf{x}(t)$ from which one wants to initiate the forecast, identifying the k points $\mathbf{x}(t_i)$ ($i = 1, \dots, k$), with $t_i < t$, nearest to $\mathbf{x}(t)$ that minimize the quantity

$$\|\mathbf{x}(t) - \mathbf{x}(t_i)\|, \quad (12)$$

which constitute the set corresponding to the point $\mathbf{x}(t)$. A local map \hat{f}_T is then constructed, which has the set of the $\mathbf{x}(t_i)$ as domain and that of the $\mathbf{x}(t_i + T)$

as codomain. If, as component $x(t+T)$ interpolates the pair

As for the choice simpler than those of representations (order reaching a greater therefore of a great the literature^{25,85,93} the nearest neighbor quadratic one (third of interpolation greater dimension of the attractor of coefficients and time instead the optimum local map complexity)

In accordance with approximation, into nomials. We observe is still nonlinear because a different neighborhood of \hat{f}_T .

We also note that order to determine $k_{\text{min}} = (m+g)/(m$ which noise is present consider wider neighborhoods such a case, the pro

with the least squares the matrix of the variance heaviest computational more efficient using

In the process of with the method proposed or rather a simplification it entails the isolation of $m+1$ neighbors contained inside it and the distance from $\mathbf{x}(t)$.³

as codomain. If, as is often happens, we are only interested in forecasting the last component $x(t+T)$ of $\mathbf{x}(t+T)$, the search is limited to a map $\hat{f}_T : \mathfrak{R}^m \Rightarrow \mathfrak{R}$, which interpolates the pairs $(\mathbf{x}(t_i), x(t_i+T))$ instead of a function $f_T : \mathfrak{R}^m \Rightarrow \mathfrak{R}^m$.

As for the choice of the function \hat{f}_T , one may use expressions which are much simpler than those considered in the global approximation. If we consider high order representations (order refers to the derivative on which mostly the error depends²⁴), reaching a greater flexibility requires neighborhoods of greater dimensions, and therefore of a greater complexity to reproduce. Essentially all the applications in the literature^{25,85,93} stop at the third order and therefore consider three possibilities: the nearest neighbor (first order), the linear approximation (second order), and the quadratic one (third order). Whilst in the case of low-dimensional chaos, orders of interpolation greater than 3 can bring improvements, with the growth of the dimension of the attractor, due to the fact that larger orders require a higher number of coefficients and therefore larger neighborhoods, orders equal to 2 or 3 constitute instead the optimum choice,²⁵ that is the best compromise between set size and local map complexity.

In accordance with this, in the present approach we consider a second order approximation, interpolating the pairs $(\mathbf{x}(t_i), x(t_i+T))$ with 1st degree polynomials. We observe that even if the approximation \hat{f}_T is linear, the prediction is still nonlinear because during the forecast procedure every point corresponds to a different neighborhood, and therefore to different neighbors and different expressions of \hat{f}_T .

We also note that, even if the minimum number of neighbors to be identified in order to determine the approximation parameters with polynomials of degree g is $k_{\min} = (m+g)!/(m!g!)$, it is often useful, particularly in the case of time series in which noise is present (a circumstance which always happens in natural series), to consider wider neighborhoods in order to give better stability to the forecast. In such a case, the problem of interpolation can be solved by minimizing the error

$$e = \sum_{i=1}^k \|x(t_i+T) - \hat{f}_T(\mathbf{x}(t_i))\|, \quad (13)$$

with the least squares method,⁸⁴ as is done in the present work, or by factorizing the matrix of the values $\mathbf{x}(t_i)$.⁹³ Search of the k neighbors, which constitutes the heaviest computational burden in local approximation methods, can be made much more efficient using the algorithm already mentioned proposed by Grassberger.³¹

In the process of identification of the function \hat{f}_T , we have also experimented with the method proposed by Sugihara and May,⁸⁵ which constitutes a modification, or rather a simplification, of that of Farmer and Sidorowich.²⁴ Contrary to the latter, it entails the isolation in embedding space of a simplex, identified by $k = k_{\min} = m+1$ neighbors constituting its vertices, chosen in such a way that the point $\mathbf{x}(t)$ is inside it and the weighing, in the forecast, of each neighbor is in relation to the distance from $\mathbf{x}(t)$.³¹ However, this method leads to results which on average are

worse than those obtained by the method of Farmer and Sidorowich. This may be attributed to the choice $k = k_{\min}$ which, despite the weights, does not provide any way to reduce the negative effect of noise.

The forecast is generally made by choosing $T = \Delta t$, that is considering a forecast time interval equal to the sample interval of the time series. When instead the forecast is for $T = n\Delta t$ (with $n > 1$), there are two possible schemes: iterated forecast and direct forecast.^{24,25} With the former scheme one evaluates the map for Δt and then iterates it $(n - 1)$ times until it reaches time T . With the latter procedure a new map is constructed to approximate f_T at each time T . Farmer and Sidorowich show that when the local approximations are well identified, the iterated method provides better forecasts.

At the beginning of this section we emphasized how the importance of nonlinear prediction resides also in helping one to discern between dynamics which, even though different, can produce time series very similar in appearance and difficult to distinguish. Such a potential capacity makes nonlinear prediction a precious investigative instrument, almost independently of its predictive aspect, when searching for indications of a chaotic dynamics in complex time series.

For this purpose, several authors^{22,66,85,96} suggest that the forecast as far as its predictive step T is concerned, should enable us to distinguish periodic and quasi periodic signals (in which the quality of the forecast, though elevated, remains constant or oscillates with T) from chaotic ones (in which case it decreases in a monotonic manner, due to the progressive divergence of the trajectories in phase space, linked to positive Lyapunov exponents).

Moreover, nonlinear prediction also constitutes an important instrument to distinguish chaotic signals from stochastic ones, whether or not with zero autocorrelation. In the first case, whilst for a white noise the predictive capacity remains at low levels and is almost constant with the growth of T , when the signal is chaotic the quality of the prediction cannot but decrease.^{85,93,97} This is also true when the non-correlated stochastic signal is superimposed on a periodic or quasi periodic signal,^{85,93} in which case the correlation between real series and forecast series again remains constant or oscillates, but now around a value linked to the noise present.

When there is nonvanishing autocorrelation the question is much more delicate. As mentioned in Sec. 3, several works,^{60,72,89} have demonstrated the capacity of some types of colored noises, e.g. fractal Brownian motions (characterized by a spectrum of the form $S(f) = Cf^{-\alpha}$), to mimic certain characteristics of chaotic signals. With regard to this, Tsonis and Elsner⁹⁵ have highlighted a further aspect of nonlinear prediction: as the forecast time interval changes, the accuracy of the forecast decreases according to a different law, depending on whether the signal is chaotic or fBm. In the former case, the dependence between the correlation coefficient

$$r = \frac{\overline{x_r x_p} - \bar{x}_r \bar{x}_p}{\sigma_r \sigma_p} \quad (14)$$

(with subscripts r and p) is the following

where $s(0)$ is a measure of the correlation and K is a lower bound

where H is the Hurst exponent and D is the dimension of the attractor, w_i are the weights

Therefore, in practice, the correlation coefficient is assumed to have the form

A further capacity of nonlinear prediction is that, up to now we have not been able to correctly embed a time series. We apply it to a time series by trial and error until we find a time interval τ which allows the identification of the attractor. It is also true that such a procedure is not an optimum phase space search. It has been indeed noted that there are doubts regarding the validity of the method. It is actually plausible that there are time intervals τ which are not optimal. The criteria noted above are not sufficient where it can happen that the identification of the dynamics, and manifold as time increases.

In conclusion, the method is formally similar, but it is not proposed in statistical terms. The local linear method provides an improvement on the method.

The latter method was proposed by Karlsson and

We finally cite the work of Holubeshen⁴⁴ in which it is shown that this paper is concerned with the identification of a chaotic dynamical system.

(with subscripts r and p indicating the real and forecast values respectively) and T is the following

$$r(T) = 1 - \frac{s^2(0)e^{2KT}}{2\sigma_r^2}, \quad (15)$$

where $s(0)$ is a measure of the amount of information present in the initial state and K is a lower bound to the real metric entropy. For the fBm signal we have instead

$$r(T) = B \sum_{i=1}^k w_i \left(1 - \frac{i}{T}\right)^{2H}, \quad (16)$$

where H is the Hurst scale exponent (equal to the reciprocal of the fractal dimension D), w_i are the coefficients of the nonlinear prediction and B is a positive constant.

Therefore, in presence of a chaotic dynamics there is an exponential link between the correlation and the forecast time interval; whilst for an fBm the dependency assumes the form of a power law.

A further capacity of nonlinear prediction regards the embedding dimension. Up to now we have described nonlinear prediction presupposing the knowledge of the correct embedding dimension m . It is instead evident that when we want to apply it to a time series for which the value of m is not known, we must proceed by trial and error. Sugihara and May⁸⁵ not only suggest that nonlinear prediction allows the identification of the value of m which produces the best forecast, but also that such a value, revealed by a knee bend in the diagram $r = r(m)$, is the optimum phase space dimension in which to construct the attractor. Such a feature has been indeed noted by Tsonis⁹³ and Tsonis, Triantafyllou and Elsner,⁹⁷ though doubts regarding it had been expressed by Grassberger, Schreiber and Schaffrath.³⁴ It is actually plausible that good forecasts may be obtained with values of m and τ which are not optimum in the reconstruction of the attractor according to the criteria noted above. This is consistent with the local nature of nonlinear prediction, where it can happen that "non optimum" pairs of m and τ may seize some aspects of the dynamics, or of sections of the time series, especially when this is as complex and manifold as the case under consideration.

In conclusion of this section it is worth recalling that forecasting methods formally similar, or at least related, to nonlinear prediction have also been proposed in statistical fields. Among these, the threshold autoregressive method,⁹¹ the local linear method of Priestly,^{68,70} and the method of Pikovsky,⁶⁴ that is an improvement on the method of analogs proposed by Lorenz⁵¹ are especially notable.

The latter method has been used with success in particular in runoff prediction, by Karlsson and Yakowitz.^{41,42}

We finally cite, for the sake of completeness, the article by Kember, Flower and Holubeshen⁴⁴ in which nonlinear prediction is applied to the forecasting of river flow. This paper is concerned with the predictive aspect, without however investigating if a chaotic dynamics exists in the time series considered.

8. Application of Nonlinear Prediction

We discuss in this section our analysis of the time series of mean daily discharges from Tavagnasco section of the river Dora Baltea by the nonlinear prediction method, based on a local approximation of the second order. This approximation was preferred to the global one, because the natural phenomenon under study has a complex dynamics and therefore the behavior of the attractor can be expected to be more describable, in the very short term, through local methods.

It is indeed of the utmost practical importance to be able to make discharge forecasts reliable for 1–2 days, in view of possible engineering implications, and this further emphasises the advantage of choosing the methods which should provide the best short-term forecasts.

Also, the test proposed by Tsonis and Elsner, related to the possibility of discerning between chaotic signals and fBm, refers to the very first predictive steps; therefore, since local methods in this case enable better forecasts, we believe that this test should be more precise if done using such methods.

In applying nonlinear prediction to the time series available, the first 13000 days (from 1st January 1941 to 4th August 1976) were considered as reference time series, in such a way that the attractor could be explored as comprehensively as possible given the length of the series available. The subsequent 200 days were overlooked (to avoid the possibility of direct consequentiality between the base series and the series to predict) and the forecasts were realized with reference to the 300 days from 21st February 1977 to 17th December 1977.

The 300 values used to forecast may appear not numerous enough in view of the stability of our results. However this constitutes the best compromise between a good attractor description (contained in the reference series) and a sensible significance of results (linked precisely to the length of the forecasted series). The complexity of the natural phenomenon under study motivates of course the high number of values constituting the first series.

Figure 14 shows the portion of the signal considered for the forecast. It well represents the entire series available, exhibiting the principal characteristics (intense floods which graft themselves onto the basic dynamics). We note in particular that in the second part a phenomenon appears which is unusual with respect to the thirty-year history available: two very intense floods (having maximum mean daily discharges equal to about 14 and 13 times the mean of the series and about 16 and 13 times the mean square deviation, respectively) occurred within a very short time interval (the first took place on 30th September 1977, the second on 8th October 1977).

We considered embedding dimensions m variable from 4 to 20, each of which was explored, with $T = \Delta t = 1$ day, using delay times τ ranging from 1 to 6, with unitary scansion (namely, from 6 to 30, considering multiples of 3). In such a way we wanted to study in large detail how the forecast quality is influenced by

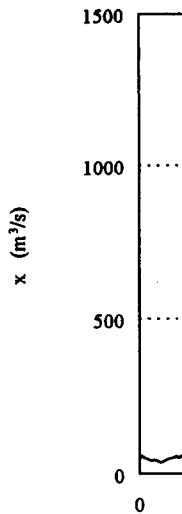


Fig. 1

the choice of the time series, the differences and differences in the attractor.

As for the number of values used to forecast, k was varied from 1 to 300 to find the optimum. For higher values of k , the wider neighborhood of the attractor and consequently the forecast is less stable as k is increased. The forecast (due to the least squares method) was investigated the possible advantages of the attractor considered.

Figure 15 shows the behavior of the attractor. The behavior appears irregular. The attractor of the sort considered is of the sort considered. The surface is obtained. The behavior, two important characteristics decrease with the shortest delay time considered. Second, there are values of

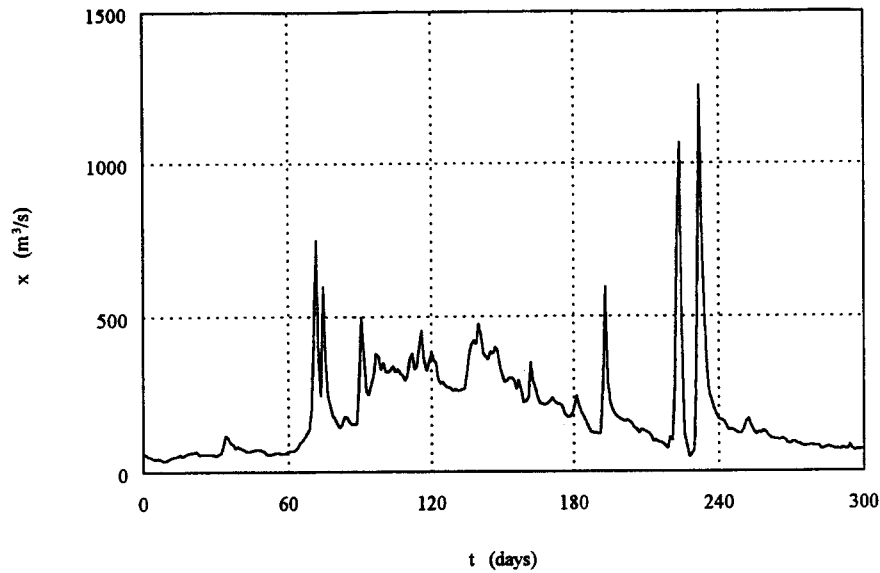


Fig. 14. Diagram of the time series considered for the forecast.

the choice of the two quantities m and τ , and to highlight possible correspondences and differences with what had emerged from the reconstruction of the attractor.

As for the number of neighbors to use, different tests, in which the value of k was varied from $k = k_{\min}$ to $k = 3m$, showed the number $k = 2m$ of neighbors to be optimum. For higher values of k , the k points become involved with increasingly wider neighborhoods for which the local model becomes increasingly less adapted, and consequently the errors grow. Below $k = 2m$ the method becomes less and less stable as k is decreased with an ever increasing number of large errors in the forecast (due to the appearance of quasi-singular matrices in the application of the least squares method adopted to minimize the error e defined in (13)). We also investigated the possibility of employing different numbers of k in various zones of the attractor considered (e.g. where there are large floods), but with no noticeable advantages.

Figure 15 shows the three-dimensional surface $r = r(m, \tau)$ thus obtained. Its behavior appears irregular, as might be expected for a complex natural phenomenon of the sort considered, and somewhat affected by noise, in view of the fact that the surface is obtained from 300 forecast values. Nevertheless, observing its mean behavior, two important features can be noticed: first of all the correlation coefficient decreases with the growth of τ , ranging from values around 0.70–0.75 for the shortest delay times to values variable around 0.5 for the largest τ among those considered. Second, still observing the mean behavior of the surface, we note that there are values of r greater than 0.65–0.70 only for τ inferior to 5–10 days, whilst

for τ larger than about 15 days r is practically always below 0.6. Both these observations appear to confirm what was observed by the reconstruction of the attractor: the optimum delay time is found for τ of the order of units (in particular the nonlinear prediction would indicate $\tau = 1-2$ days), while values above about 10 days lead on average to increasingly worse forecasts.

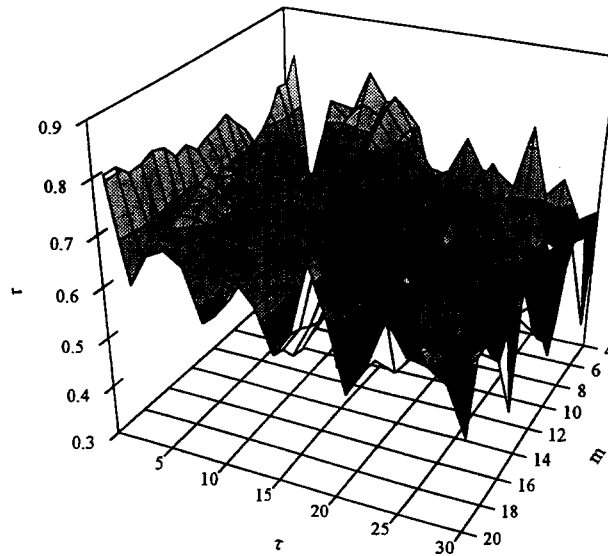


Fig. 15. Correlation coefficient behavior versus embedding dimension and delay time.

Preliminary tests for some pairs (m, τ) , considering 600 forecast values, have reproduced substantially the strong irregularities visible in Fig. 15.

Peaks can be observed, which dramatically raise locally the quality of the forecast with respect to the surrounding pairs (m, τ) , and pronounced minima which on the contrary create sharp falls in r . Furthermore we note that the peaks tend to accumulate mainly along lines with constant τ , in particular for $\tau = 12, 18$ and 24 days, pointing out to a certain regularity which is reminiscent of the periodicities observed in the results on the maximum spreading of trajectories.

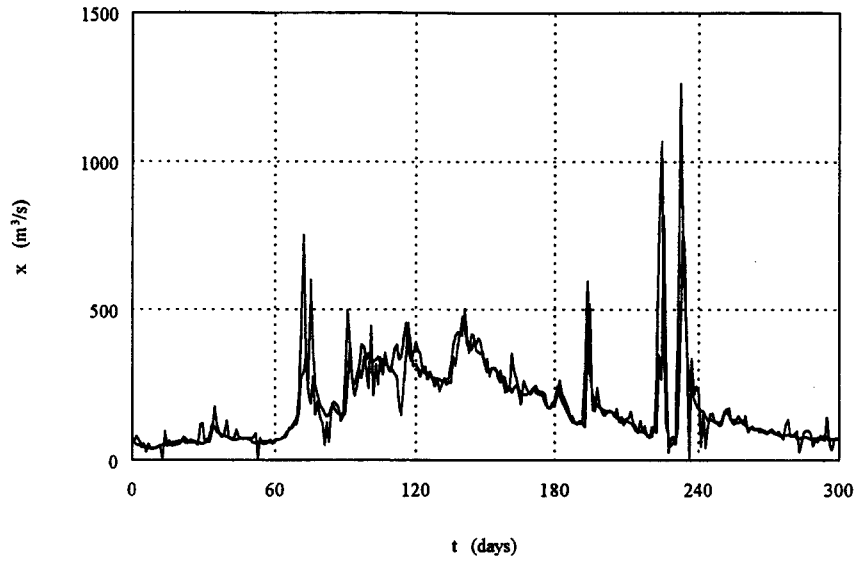
Observing the surface through lines $\tau = \text{constant}$ in order to investigate the shape of the link between the correlation coefficient and the embedding dimension, one cannot clearly identify a particular behavior, either regular or characteristic, and it appears hardly possible to have indications on values of m enabling, on average, better forecasts. Consequently, indications on the value of the optimum embedding dimension for the reconstruction of the attractor cannot be deduced from this analysis. There is therefore no way to confirm what was deduced by the evaluation of the correlation integral, where a slight saturation beginning from m of about 5-6 seemed to emerge.



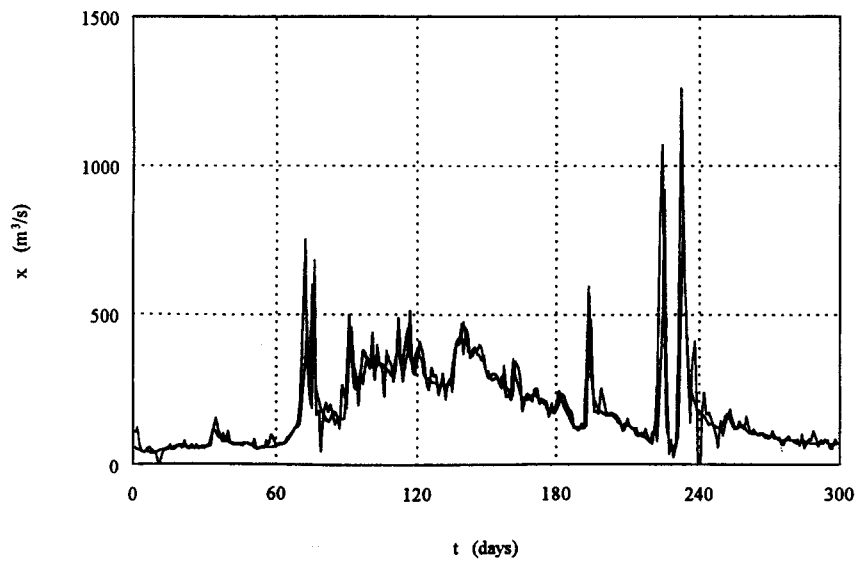
Fig. 16. Comparison between (a) $m = 18, \tau = 1$ day.

In order to exemplify the comparison between

Both these
ion of the at-
in particular
ove about 10



(a)



(b)

Fig. 16. Comparison between the real time series and that forecast. (a): $m = 12$, $\tau = 1$ day; (b): $m = 18$, $\tau = 1$ day.

lay time.
values, have
f the forecast
na which on
eaks tend to
2, 18 and 24
periodicities

investigate the
g dimension,
characteristic,
enabling, on
he optimum
be deduced
duced by the
aing from m

In order to exemplify which kind of forecast is synthesized by a value corresponding to the shortest delay times of r of about 0.70–0.75, Figs. 16a–b show the comparison between the real series and the forecast series, adopting $m = 12$ and

$m = 18$, respectively, both with $\tau = 1$ day (the relative values of the correlation coefficient are 0.77 and 0.79). Recalling that this is a natural phenomenon in which noise is present, the result of the nonlinear forecast can be certainly considered good. In fact, not only is the average behavior well forecasted, but some insight into several aspects of great hydrological importance is also gained: the main sign inversions of the time derivative and the localization, the duration, and, with an error still tolerable from an engineering point of view, the maximum values of the floods. However, the presence of spurious oscillations should also be noted in the forecast series, with a characteristic increase in the amplitude corresponding to the depletion curves of the most powerful floods.

In order to understand if large isolated mistakes (which sometimes, though rarely, may appear in the forecast, due to the presence of tangent trajectories in the phase space) are what makes the surface $r = r(m, \tau)$ so irregular, the 30 worst values of the series (equal to 10% of the total) were excluded in the calculation of the correlation coefficient (in accord with what is reported in other works (e.g., Refs. 10 and 50).

Figure 17 shows the corresponding new surface $r = r(m, \tau)$. The surface has now a behavior on average more regular than the previous one, mainly for τ less than about 15 days, and some of the irregularities have disappeared, or at least have been strongly reduced (such as, e.g., the minimum observed in the neighborhood of $m = 4$ with $\tau = 4$). Besides, we now see more clearly that the mean behavior decreases with the growth of the delay time: from values of r about 0.9 for $\tau = 1-2$ days, to r of about 0.60-0.65 for $\tau = 27-30$ days.

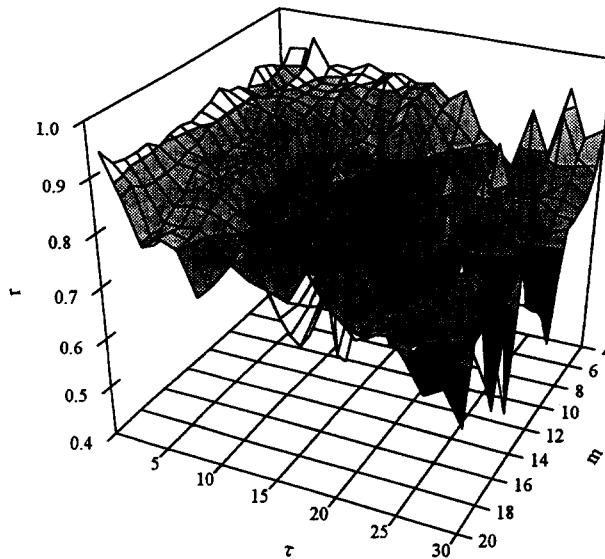


Fig. 17. Correlation coefficient behavior versus embedding dimension and delay time, excluding the 30 worst forecasts (equal to 10% of the total).

One feature we note, with decreasing m to the surface of r (and hence values of τ provided small m can be guessed from

A possible expectation of r is the following: values of 4-6 days, a better description of those methods ($r = r(m)$). Coming from the high values, less and less specific case to days, its extreme or such link to effect of the $r = r(m, \tau)$.

Proceeding between the corresponding dimension equal to that were obtained

Figure 18 growth of T is observed in that the sign combination

With regard to signal from a semilogarithmic in this case, values. In fact on which of that its behavior forcing r to appear trends: it would Δt considered. Nevertheless,

es of the correlation phenomenon in which certainly considered ed, but some insight ed: the main sign in- n, and, with an error values of the floods. e noted in the fore- corresponding to the

sometimes, though agent trajectories in regular, the 30 worst d in the calculation in other works (e.g.,

τ). The surface has ae, mainly for τ less are, or at least have n the neighborhood ; the mean behavior out 0.9 for $\tau = 1-2$

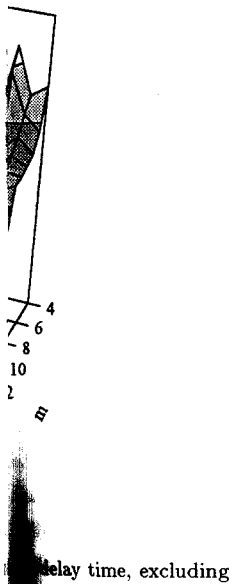
One feature of the surface stands out: looking at it along the lines $\tau = \text{constant}$, we note, with the exception of the very first values of delay time, a behavior always decreasing on average with the growth of the embedding dimension m , which gives to the surface an amphitheatre shape. This implies that on average the same values of r (and hence the same quality of the forecast) which are obtained with certain values of τ for m larger than about 10, are also possible for larger values of τ , provided small m are selected. Even if less evident, a similar behavior can already be guessed from the original surface $r = r(m, \tau)$.

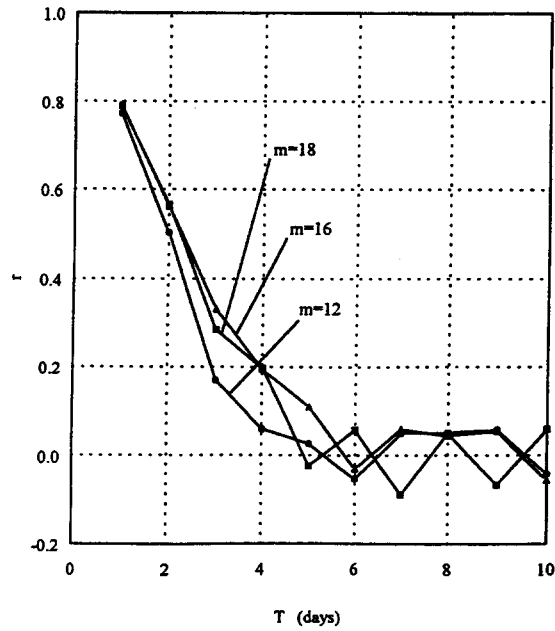
A possible explanation of this feature, which would seem to contradict the expectation of r initially growing with m and then remaining essentially stable,^{85,93} is the following. It is true that the growth of the embedding dimension m from values of 4-6 to larger values, should progressively "reveal" the attractor, enabling a better description of it and therefore better forecasts (this concept is at the basis of those methods seeking the correct embedding dimension by looking at the link $r = r(m)$). On the other hand, it is also true that with the growth of τ , starting from the highest values of m , the extreme components of the vector $\mathbf{x}(t)$ become less and less dynamically linked, with the consequent risk of irrelevance. In this specific case there are doubts on whether, when the vector $\mathbf{x}(t)$ covers many tens of days, its extremities are still dynamically linked (particularly regarding the floods) or such link is not disguised by noise. This could then combine with the positive effect of the growth of m , justifying, at least in part, the behavior of the surface $r = r(m, \tau)$.

Proceeding now to forecasts over several days ($T > \Delta t$), Fig. 18a shows the link between the correlation coefficient and the forecast time interval relative to embedding dimensions 12 and 18, and $\tau = 1$. The behavior in such figure is qualitatively equal to that identified for all the other values of m and τ considered. The forecasts were obtained with iterative technique.

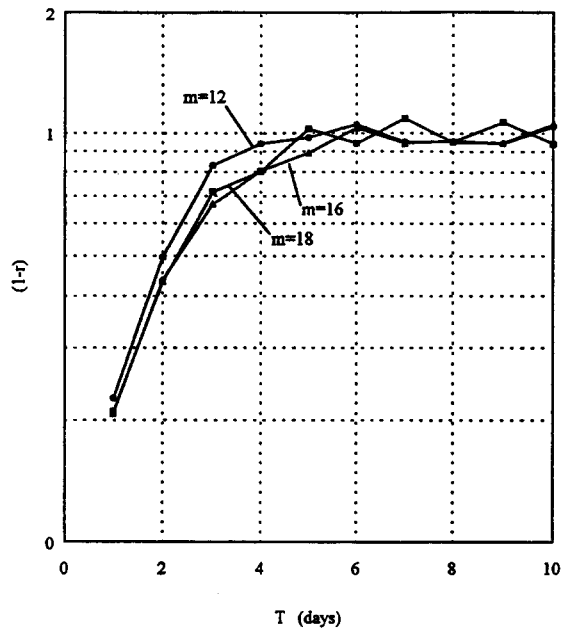
Figure 18a shows that the capacity to make forecasts falls rapidly with the growth of T and does not show significant oscillations. This is in accord with what is observed in time series generated by chaotic dynamics, and agrees with the fact that the signal analyzed comes neither from a periodic phenomenon nor from a combination of a periodic with a non-autocorrelated stochastic signal.

With regard to the test proposed by Tsonis and Elsner to distinguish a chaotic signal from an fBm, the values of $(1 - r)$ versus the forecast time are shown on the semilogarithmic plane (Fig. 18b). The plot shows that the test cannot be decisive in this case, since the zone of interest is practically reduced to only the first three values. In fact, at T equal to about $4\Delta t$, the coefficient correlation, independently on which of the two dynamics has generated it, has already reached values so low that its behavior for larger T cannot but be squeezed onto the line $\log(1 - r) = 0$, forcing r to approach zero for both. Consequently, it is rather arbitrary to judge such trends: it would rather be necessary to investigate smaller fractions of the interval Δt considered here, in order to have a more extensive section of significant curve. Nevertheless, even with the above caution, the identifiable trend is increasingly close





(a)



(b)

Fig. 18. Correlation coefficient behavior versus forecast interval. (a)–(b): original series; (c): series minus the 10%.

to a straight form.

Such a by excluding where we s formula (1.

Comme mentioned dom compo under vario presence of pletely cap not very h maximum value properly at

For this the origina of the cha however, th than harm

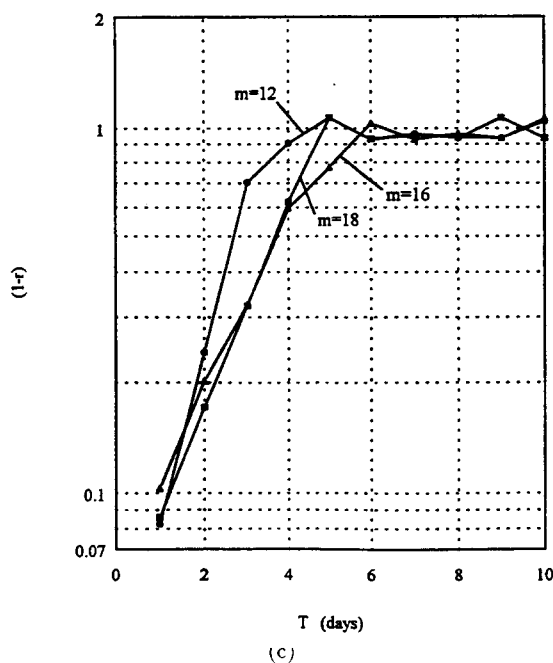


Fig. 18. (Continued)

to a straight line, which makes us believe that the law $r = r(T)$ is of the exponential form.

Such a law emerges more clearly if the test is applied to the series obtained by excluding the 30 worst forecasts. The relative behaviors are shown in Fig. 18c, where we see that the initial part now comes much closer to a straight line, as the formula (15) would imply.

Commenting on the results obtained up to now, the presence of noise has been mentioned many times; intending by noise either the existence of a possible random component superimposed on the chaotic deterministic one, or noise introduced under various forms by the measuring operation, or, even more likely, the possible presence of some higher-dimensional chaotic dynamics, which would not be completely captured by the methods adopted here. It is believed that the good but not very high values of r , and perhaps also the impossibility to discern some optimum value for the embedding dimension of the attractor, can be, at least in part, properly attributable to such a fact.

For this reason we decided to apply a filtering, based on the usual techniques, to the original signal. Even though this may involve a partial destruction or alteration of the chaotic dynamics possibly present in the original signal,^{2,12,15,34} we expect, however, that filtering should, in the case of nonlinear forecasts, be more beneficial than harmful, as suggested by experiments⁵⁵ as well as by theoretical arguments.¹²

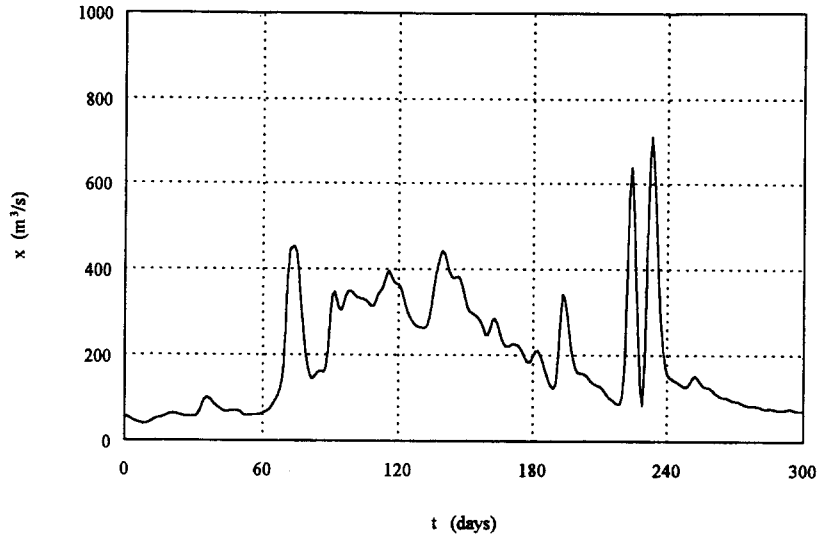


Fig. 19. Diagram of the time series to predict, after the filtering.

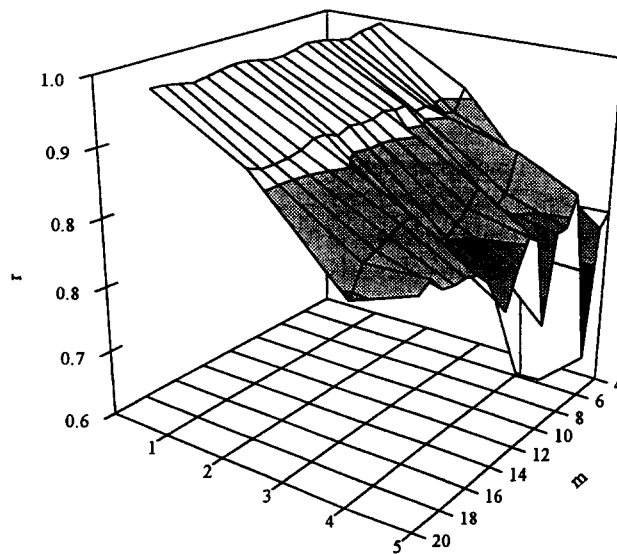


Fig. 20. Correlation coefficient behavior versus embedding dimension and delay time, for the filtered series.

Despite the difficulty of establishing the noise characteristics *a priori*, it is plausible to assume that its effect is localized not only at high frequencies, but has on the contrary a wide frequency extension: consequently we decided to adopt a filter (Butterworth) that operates weakly on all frequencies above 0.04 days^{-1} .

The effect of the series of the filter that even though variations of small amplitude, from the principal behavior point of view, the series is certainly interesting.

The same type of original series. For $r(m, \tau)$, evaluated at times up to 5. For an interval T , for m

Fig. 21. Correla

The first of the of all, the values are exceptionally close to a natural series. For the forecast value $\tau = 1$, representing The forecast is in of $T = 1$ day and

The effect of the filtering is shown in Fig. 19, which provides details of the time series of the filtered forecast. Comparing it with the original (Fig. 14), we note that even though the behavior is much more regular now and the rapid oscillations of small amplitude have disappeared, the filtered series reproduces very well the principal behavior of the discharges, including the floods. From an engineering point of view, the possibility to make reliable forecasts on the filtered series remains certainly interesting.

The same type of investigation was conducted on the filtered signal as on the original series. Figure 20 shows the behavior of the correlation coefficient $r = r(m, \tau)$, evaluated for the same value of m indicated before, but now with delay times up to 5. Figure 21 shows the forecast behavior versus the forecast time interval T , for $m = 12$ and $m = 18$ ($\tau = 1$).

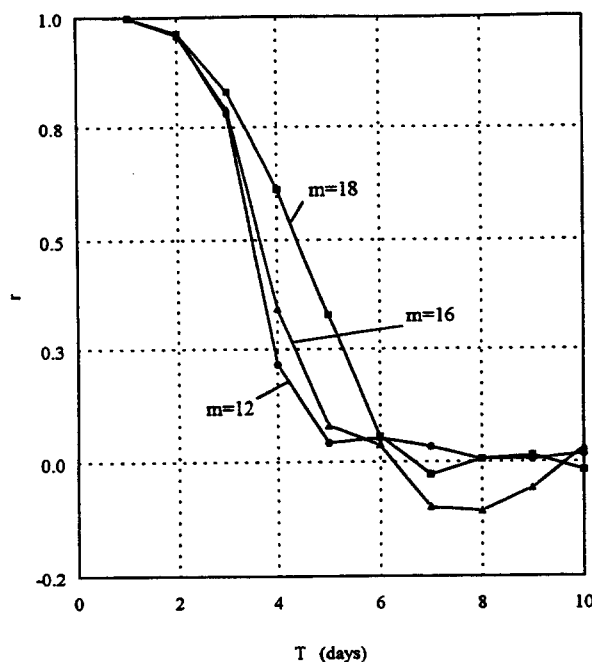
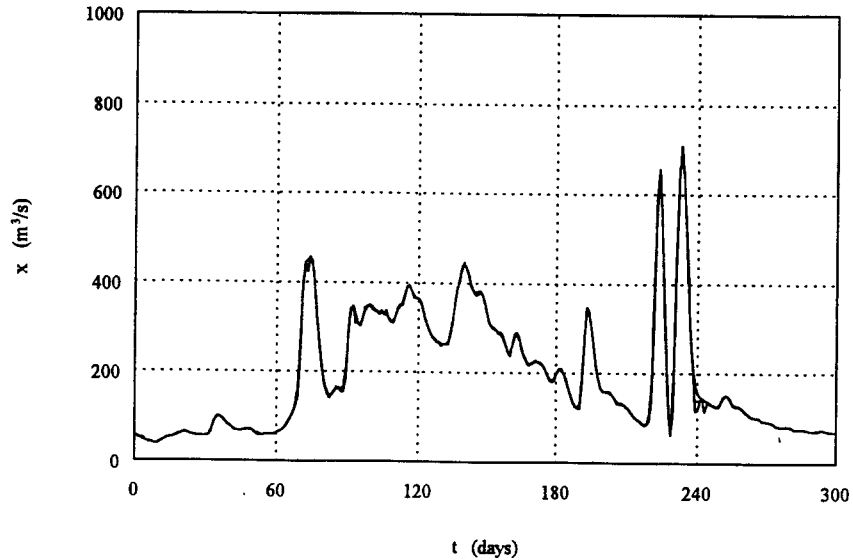
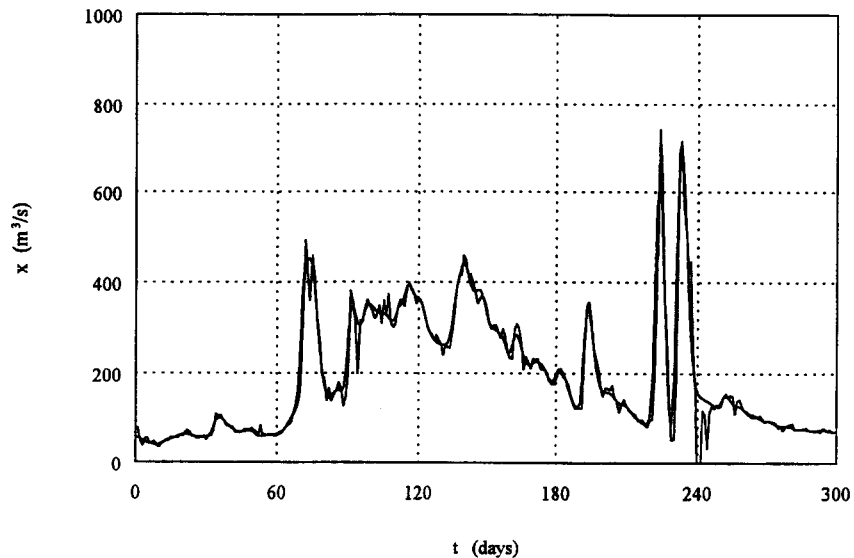


Fig. 21. Correlation coefficient behavior versus forecast interval, for the filtered series.

The first of the two figures shows aspects which are worth commenting on. First of all, the values of r have become very high and for $\tau = 1$ and $\tau = 2$ they are exceptionally close to 1 (r assumes values around 0.998 and 0.975 respectively) for a natural series. Figures 22a-b show the comparisons between the real values and the forecast values for $T = \Delta t = 1$ day and $T = 2\Delta t = 2$ days, with $m = 18$, and $\tau = 1$, representatives of common behavior for other embedding dimensions as well. The forecast is impressively good: the lines are practically coincident in the case of $T = 1$ day and very close for $T = 2$ days. To be noted in particular the fact



(a)



(b)

Fig. 22. Comparison between the filtered real time series and that forecast. (a): $m = 18$, $\tau = 1$ day, $T = 1$ day; (b): $m = 18$, $\tau = 1$ day, $T = 2$ days.

that the unusual double flood peak, mentioned earlier, is not altered substantially by the filtering and is perfectly reproduced in each part. Furthermore, the forecast catches very well all the sign changes of the time derivative of the series, the form

of the floods, earlier have c

Moreover, ones, while for some preliminary irregular behavior series. We note axis more marked $\tau = 1$ day and here instead we conclude that the choice of

Looking in weak for $\tau =$ to have a certain not show a kn

If we now find the same descending behavior strong resemblance model,⁹⁶ following relations.

Finally, in nonlinear pre also on the two a test analogous found with re in relation to

9. Summary

Even though regarding the of the behavior to believe th considered.

The fill-fa order to obtain substantial a 4–5, and on the maximum 5–6

The attract for $\tau = 1$ and

of the floods, and the maximum and minimum values, whilst the oscillations noted earlier have completely disappeared.

Moreover, up to $\tau = 3$ days the surface is much more regular than the previous ones, while for τ equal to 4 and 5 days we observe sharp and strong oscillations which some preliminary tests, not reported here, show to be the prelude to a generally irregular behavior for higher τ , qualitatively similar to that verified for the original series. We note also that the surface exhibits a descending behavior along the time axis more marked than those noted in the original series. In the latter, between $\tau = 1$ day and $\tau = 5$ days, r is on average nearly constant with small variations; here instead it passes from about 0.998 to a mean value around 0.6. From this we conclude that the quality of the forecast is in present case much more sensitive to the choice of τ .

Looking in detail at the behavior of r versus m we observe oscillations that are weak for $\tau = 1-3$ days, much stronger for the remaining two delay times, and appear to have a certain regularity in time. The filtered series, like the original one, does not show a knee bend which would reveal the optimum m .

If we now consider the dependence of r versus the forecast time (Fig. 21), we find the same type of link $r = r(T)$ observed in the original series: monotonic descending behavior, very similar to that noted in chaotic dynamics (notice the strong resemblance with what was obtained for the logistic map and the Lorenz model,⁹⁶ followed by values very close to zero and not affected by significant oscillations.

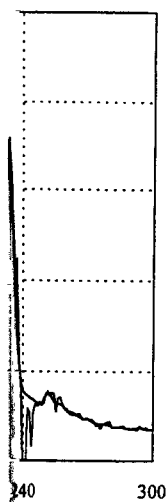
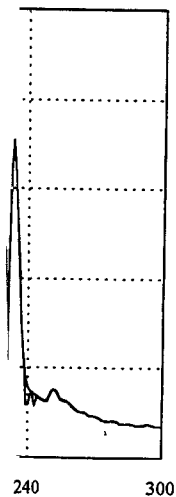
Finally, in order to investigate the influence of autocorrelation on the results of nonlinear prediction, part of the elaborations described up to now were repeated also on the two signals obtained differencing the original series and the filtered one: a test analogous to those already carried out in Sec. 6. No substantial difference is found with respect to the original series, and the forecasts appear to be analogous in relation to m , τ and T as well.

9. Summary of Results and Conclusions

Even though this work does not allow us to conclude with a definitive answer regarding the possibility whether a chaotic dynamics is or is not at the basis of the behavior of runoff in a natural water course, the following facts lead us to believe that a strong deterministic component does exist in the time series considered.

The fill-factor and the maximum spreading of trajectories methods, used in order to obtain indications for the correct reconstruction of the attractor, show a substantial accord both on the embedding dimension, which must be higher than 4-5, and on the delay time, where the range of choice is restricted to a few days, maximum 5-6.

The attractors subsequently reconstructed by Takens' method, exhibit especially for $\tau = 1$ and 2 days, the presence of a quite evident ordered structure.



(a): $m = 18, \tau = 1$

ered substantially
more, the forecast
e series, the form

With the growth of τ , in particular when values are chosen of 8–10 days, in analogy to what is observed in the results based on nonlinear prediction, the behavior of the fill factor, of $P_m(\tau, r)$ and of the correlation integral become gradually similar to those typical of a casual signal. This is typical of chaotic signals, which are dynamically linked to short time values but become practically independent for long times.

Still more characteristic is the behavior of the correlation integral slopes, which shows a point of inflection more or less horizontal in the central zone separating the effect of depopulation on one side and that of saturation and noise on the other. The values of the slope in this zone are always below 4. Furthermore, even if a real “plateau” does not exist and saturation is not complete, the behavior tends increasingly to the horizontal with the growth of the embedding dimension, especially for values of m above 5–6 (Fig. 10). This constitutes an indication of the possible existence of deterministic chaos in the series.

Finally, also the result of tests performed on the first difference signal, in order to verify if what was observed on the original signal could be possibly due to its degree of autocorrelation for short time intervals, are very significant. Having checked that the characteristic quantities of the difference signal are analogous to those of the original one, we believe that what was observed on the discharge series may effectively be due to the dynamics of the phenomenon and not to simple autocorrelations.

The application of nonlinear prediction has produced several positive results. First of all, the good quality of the forecast emerges: the examples shown in Figs. 16a–b, together with the correlation coefficient values oscillating around 0.75, testify that the mean behavior of the phenomenon is forecasted with reliability in all its principal hydrological characteristics (local trends, position and form of floods, sign inversion of the time derivative). Such forecasts are even more impressive if we consider the complexity of the natural phenomenon investigated, and the fact that the forecasts leave out of consideration any hydrological information relative both to the inflow on the basin and the basin itself, and are obtained by looking only at the dynamical history of the variable considered. This latter observation has important implications, in that it suggests that the series has in itself trace of all the variables which are involved in the complex dynamics. One can see here a confirmation of the delay-time technique of Takens.

Even though the study of the influence of m and τ does not give clear indications for the optimum choice of the embedding dimension, detailed as it may be with regard to the delay time, it confirms instead the substance of what was observed in the reconstruction of the attractor, namely that the optimum values of τ are of the order of units. As for the quality of the forecast, it is found that exclusion of the worst 10% raises the correlation coefficient to about 0.9.

The second positive result of nonlinear prediction is the behavior of the predictive capacity with respect to the forecast interval. At the growth of the latter

the former decl
the two may b
we are either i
added to a pe
Brownian moti
the forecast m
becomes more

With the ca
of the forecasts
and real values
of two days, aft
in the dynamic
strong determi
the first differ

Beside thes
investigation.
the course of th
adopted is cert
It is perhaps il
vastness the sin
pect that, prov
dynamics. Ext
the intermitten
diagnosis of cha

We may sa
now has given
(rather, they er
experiment wit
precise.

With regard
directions: the
for chaotic syst
present analysi
data technique

Besides wor
models allowin
surface and un
dynamics. Suc
hydrological fa
capacities, acq
when the forme
results with the
series.^{6,29,40,77}

the former declines rapidly, and we do not observe oscillations; the relation between the two may be considered exponential. This should exclude the possibility that we are either in the presence of a stochastic signal with correlation zero, possibly added to a periodic or quasi periodic one, or that we are dealing with a fractal Brownian motion. The latter account is reinforced when we take into consideration the forecast minus its worst 10%, for which the fall of r with the forecast interval becomes more markedly exponential.

With the careful application of a weak filtering on the original series the results of the forecasts remain very good, and the correspondence between forecast values and real values is striking ($r = 0.998$ for one-day forecasts and $r = 0.975$ for those of two days, after which the forecasts decline sharply) also for very rare phenomena in the dynamics of the series. This seems to confirm the presence in the series of a strong deterministic dynamics component. Finally, nonlinear prediction applied to the first difference signal confirms all the previous results.

Beside these encouraging results there are as well aspects which require further investigation. The first is undoubtedly the effect of noise in the series. As noted in the course of the work, the distorting effects that noise can have on all the methods adopted is certainly important. There is then the complexity of the phenomenon. It is perhaps illusory to try and identify in a natural physical phenomenon of such vastness the single presence of a chaotic dynamics; one should possibly rather expect that, provided it really exists, such dynamics interacts with other types of dynamics. Extraneous dynamics, in our case principally the seasonal character and the intermittency, can have unexpected influence on the methods designed for the diagnosis of chaos.

We may say that if on the one hand none of the analyses conducted up to now has given place to possible exclusion of the existence of deterministic chaos (rather, they enforce just the contrary proposition), on the other it is necessary to experiment with new methods of investigation to make the dynamical picture more precise.

With regard to this latter aspect, future developments are to be expected in two directions: the application of techniques of noise reduction, specifically proposed for chaotic systems,^{13,17,26,35,45,46,54,78,79} and the reinforcement of the outcome of present analysis, verifying the existence of a nonlinear dynamics also with surrogate data techniques^{73,90} and redundancy technique.^{62,67}

Besides work should be done on the construction and analysis of conceptual models allowing us to account for how a river basin (considered in its entirety, both surface and underground) interacts with rainfall, giving possible rise to a chaotic dynamics. Such models should provide a qualitative estimate, at least, of how hydrological factors (topology of the river network, effect of lamination by storage capacities, aquifers, snowfalls) may interfere with the inflow-runoff mechanism when the former is supposed chaotic, thus providing also the tool for comparing the results with those obtained trying to extract the dynamical equations from the time series.^{6,29,40,77} We plan as well to extend the analysis to time series corresponding

to different sections of a single water course, and to rivers belonging to different pluvial systems, characterized by different networks.

We conclude by recalling the aspect which constitutes perhaps the strongest motivation for the research undertaken here: the fact that, if a chaotic dynamics is confirmed, it can provide a relevant help in realizing effective forecast of floods. In such a case, the techniques of nonlinear prediction, possibly accompanied by further refinements and combined with information on inflow,^{10,11} could be of extreme importance for both engineering and civil protection.

Acknowledgments

We thank Professor Mario Rasetti for his valuable teachings, and Professors Luigi Butera and Sebastiano Sordo for their advice, ideas and trust.

References

1. D. I. Angelbeck and R. Y. Minkara, *Journal of Environmental Engineering* (ASCE, 1993).
2. R. Badii, B. Broggi, B. Derighetti, M. Ravani, S. Ciliberto, A. Politi and M. A. Rubio, *Phys. Rev. Lett.* **60**, 979 (1988).
3. E. B. Bartlett, *Chaos, Solitons & Fractals* **1**, 413 (1991).
4. G. E. P. Box and G. M. Jenkins, *Time Series Analysis* (Holden-day, San Francisco, 1976).
5. A. Brandstätter and H. L. Swinney, *Phys. Rev.* **A35**, 2207 (1987).
6. J. L. Breeden and A. Hübler, *Phys. Rev.* **A42**, 5817 (1990).
7. Th. Buzug and G. Pfister, *Phys. Rev.* **A45**, 7073 (1992).
8. Th. Buzug and G. Pfister, *Physica* **D58**, 127 (1992).
9. Th. Buzug, T. Reimers and G. Pfister, *Europhys. Lett.* **13**, 605 (1990).
10. M. Casdagli, *Physica* **D35**, 335 (1989).
11. M. Casdagli, S. Eubank, J. D. Farmer, J. Gibson, D. Des Jardins, N. Hunter and J. Theiler, *Nonlinear Modeling of Chaotic Time Series: Theory and Applications* (Los Alamos National Laboratories, LA-UR-91-1637, 1990).
12. M. Casdagli, S. Eubank, J. D. Farmer and J. Gibson, *Physica* **D51**, 52 (1991).
13. R. Cawley and H. Guan-Hsong, *Phys. Lett.* **A166**, 188 (1992).
14. C. Chatfield, *The Analysis of Time Series* (Chapman and Hall, London, 1984).
15. A. Chennaoui, K. Pawelzik, W. Liebert, H. G. Schuster and G. Pfister, *Phys. Rev.* **A41**, 8; 4151 (1990).
16. J. P. Crutchfield and B. S. McNamara, *Complex Systems* **1**, 417 (1987).
17. M. Davies, *Physica* **D79**, 174 (1994).
18. J. Deppish, H.-U. Bauer and T. Geisel, *Phys. Lett.* **A158**, 57 (1991).
19. A. Destexste, J. A. Sepulchre and A. Babloyantz, *Phys. Lett.* **A132**, 101 (1988).
20. J. P. Eckman and D. Ruelle, *Rev. Mod. Phys.* **57**, 617 (1985).
21. J. B. Elsner, *J. Phys. A: Math. Gen.* **25**, 843 (1992).
22. J. B. Elsner and A. A. Tsonis, *Bulletin American Meteorological Society* **71**, 1; 49 (1992).
23. J. D. Farmer, E. Jen and P. J. Crutchfield, *Phys. Rev. Lett.* **51**, 1442 (1983).
24. J. D. Farmer and J. J. Sidorowich, *Phys. Rev. Lett.* **59**, 845 (1987).
25. J. D. Farmer and J. J. Sidorowich, in *Evolution, Learning and Cognition*, ed. Y. C. Lee (World Scientific, 1988).
26. J. D. Farmer
27. A. M. Frazee
28. T. W. Friso
29. G. Gouesbe
30. P. Grassber
31. P. Grassber
32. P. Grassber
33. P. Grassber
34. P. Grassber
1, 521 (199
35. S. M. Hamr
36. J. W. Havst
37. X. He and
38. H. Inaoka a
39. K. Judd, *PH*
40. K. Judd an
41. M. Karlsson
42. M. Karlsson
43. R. Katayan
Function as
Time Serie
44. G. Kember,
45. E. J. Koste
46. E. J. Koste
47. A. Lapedes
dition and
1987).
48. W. Liebert
49. W. Liebert,
50. P. S. Linsay
51. E. N. Loren
52. E. N. Loren
53. T. P. Meye
Dynamics 1
- Complexity
54. F. Mitchke,
55. M. D. Munc
56. M. A. H. N
57. C. Nicolis a
58. S. M. Omok
59. A. R. Osbo
(1986).
60. A. R. Osbo
61. N. H. Packa
712 (1980).
62. M. Palus, *F*
63. S. D. Peckh
64. A. Pikovsky
65. D. V. Pisar
66. J. M. Polyg

ging to different
 ps the strongest
 otic dynamics is
 ast of floods. In
 anied by further
 l be of extreme

Professors Luigi

gineering (ASCE,

and M. A. Rubio,

y, San Francisco,

0).

, N. Hunter and
 and Applications

52 (1991).

don, 1984).

ster, *Phys. Rev.*

37).

101 (1988).

Society 71, 1; 49

(1983).

tion, ed. Y. C.

26. J. D. Farmer and J. J. Sidorowich, *Physica* **D47**, 373 (1991).
27. A. M. Frazer and H. L. Swinney, *Phys. Rev.* **A33**, 1134 (1986).
28. T. W. Frison, *Journ. of Neural Network Computing* **2**, 31 (1990).
29. G. Gouesbet and J. Maquet, *Physica* **D58**, 202 (1992).
30. P. Grassberger, *Physica Scripta* **40**, 346 (1986).
31. P. Grassberger, *Phys. Lett.* **A148**, 63 (1991).
32. P. Grassberger and I. Procaccia, *Phys. Rev. Lett.* **50**, 346 (1983).
33. P. Grassberger and I. Procaccia, *Physica* **D9**, 189 (1983).
34. P. Grassberger, T. Schreiber and C. Schaffrath, *Int. Journ. of Bifurcation and Chaos* **1**, 521 (1991).
35. S. M. Hammel, *Phys. Lett.* **A148**, 421 (1990).
36. J. W. Havstad and C. L. Ehlers, *Phys. Rev.* **A39**, 845 (1989).
37. X. He and A. Lapedes, *Physica* **D70**, 289 (1993).
38. H. Inaoka and H. Takayasu, *Phys. Rev.* **E47**, 899 (1993).
39. K. Judd, *Physica* **D71**, 421 (1995).
40. K. Judd and A. Mees, *Physica* **D82**, 426 (1995).
41. M. Karlsson and S. Yakowitz, *Water Resources Res.* **23**, 1300 (1987).
42. M. Karlsson and S. Yakowitz, *Stochastic Hydrol. Hydraul.* **1**, 303 (1987).
43. R. Katayama, Y. Kajitani, K. Kuwata and Y. Nishida, *Self Generating Radial Basis Function as Neuro-Fuzzy Model and its Application to Nonlinear Prediction of Chaotic Time Series: IEEE* (1993).
44. G. Kember, A. C. Flower and J. Holubeshen, *Stochastic Hydrol. Hydraul.* **7**, 205 (1993).
45. E. J. Kostelich and J. A. Yorke, *Phys. Rev.* **A38**, 1649 (1988).
46. E. J. Kostelich and J. A. Yorke, *Physica* **D41**, 183 (1990).
47. A. Lapedes and R. Farber, *Nonlinear Signal Processing Using Neural Networks: Prediction and System Modeling* (Los Alamos National Laboratories, LA-UR-87-2662, 1987).
48. W. Liebert and H. G. Schuster, *Phys. Lett.* **A142**, 107 (1989).
49. W. Liebert, K. Pawelzik and H. G. Schuster, *Europhys. Lett.* **14**, 521 (1991).
50. P. S. Linsay, *Phys. Lett.* **A153**, 353 (1991).
51. E. N. Lorenz, *Journ. Atmos. Sci.* **26**, 636 (1969).
52. E. N. Lorenz, *Nature* **353**, 241 (1991).
53. T. P. Meyer and N. H. Packard, *Local Forecasting of High-Dimensional Chaotic Dynamics* in "Nonlinear modeling and forecasting", SFI Studies in the Sciences of Complexity, Proc. Vol. XII, eds. M. Casdagli and S. Eubank (Addison-Wesley, 1992).
54. F. Mitchke, *Phys. Rev.* **41**, 2; 1169 (1990).
55. M. D. Mundt, W. B. Maguire II and R. R. P. Chase, *J. Geophys. Res.* **96**, 1705 (1991).
56. M. A. H. Neremberg and C. Essex, *Phys. Rev.* **A42**, 7065 (1990).
57. C. Nicolis and G. Nicolis, *Nature* **311**, 529 (1984).
58. S. M. Omohumbro, *Complex Syst.* **1**, 273 (1987).
59. A. R. Osborne, A. D. Kirwan Jr., A. Provenzale and L. Bergamasco, *Physica* **D23**, 75 (1986).
60. A. R. Osborne and A. Provenzale, *Physica* **D35**, 357 (1989).
61. N. H. Packard, J. P. Crutchfield, J. D. Farmer and R. S. Shaw, *Phys. Rev. Lett.* **45**, 712 (1980).
62. M. Palus, *Physica* **D80**, 186 (1995).
63. S. D. Peckham, *Water Resources Res.* **31**, 1023 (1995).
64. A. Pikovsky, *Sov. J. Commun. Technol. Electron* **31**, 81 (1986).
65. D. V. Pisarenko and V. S. Pisarenko, *Phys. Lett.* **A197**, 31 (1995).
66. J. M. Polygiannakis and X. Moussas, *Solar Physics* **151**, 341 (1994).

67. D. Prichard and J. Theiler, *Physica* **D84**, 476 (1995).
68. M. B. Priestley, *Journal of Time Series Analysis* **1**, 47 (1980).
69. M. B. Priestley, *Spectral Analysis and Time Series*, Vols. I and II (Academic, London, 1981).
70. M. B. Priestley, *New Developments in Time-Series Analysis* in "New Perspectives in Theoretical and Applied Statistics", ed. P. V. Vilapiana e Wortz (John Wiley & Sons, 1987).
71. A. Provenzale, *Giornale di Fisica* **XXXIV**, 9 (1993).
72. A. Provenzale, A. R. Osborne and R. Soj, *Physica* **D47**, 361 (1991).
73. A. Provenzale, L. A. Smith, R. Vio and G. Murante, *Physica* **D58**, 31 (1992).
74. A. Provenzale, R. Vio and S. Cristiani, *The Astrophysical J.* **428**, 591 (1994).
75. A. Rinaldo, G. K. Vogel, R. Rigon and I. Rodriguez-Iturbe, *Water Resources Res.* **31**, 1119 (1995).
76. I. Rodriguez-Iturbe, F. B. De Power, M. B. Sharifi and K. P. Georgakakos, *Water Resources Res.* **25**, 1667 (1989).
77. G. Rowlands and J. C. Sprott, *Physica* **D58**, 251 (1992).
78. T. Sauer, *Physica* **D58**, 193 (1992).
79. Th. Schreiber and P. Grassberger, *Phys. Lett.* **A160**, 411 (1991).
80. H. G. Schuster, *Deterministic Chaos* (Physik Verlag, Weinheim, 1995), 3rd. edition.
81. M. Seiber, *Phys. Lett.* **A122**, 467 (1987).
82. M. B. Sharifi, K. P. Georgakakos and I. Rodriguez-Iturbe, *J. Atmos. Sci.* **47**, 888 (1990).
83. K. Stokbro and D. K. Umberger, in *Nonlinear Modeling and Forecasting*, SFI Studies in the Sciences of Complexity, Proc. Vol. XII, eds. M. Casdagli and S. Eubank (Addison-Wesley, 1992).
84. G. Strang, *Introduction to Applied Mathematics* (Wellesley-Cambridge Press, Wellesley, Massachusetts, 1986).
85. G. Sugihara and R. M. May, *Nature* **344**, 734 (1990).
86. F. Takens, *Detecting Strange Attractors in Turbulence* in "Lectures notes in Mathematics", Vol. 898 (Springer Verlag, 1981).
87. J. Theiler, *Phys. Rev.* **A34**, 2427 (1986).
88. J. Theiler, *Phys. Rev.* **A36**, 4456 (1987).
89. J. Theiler, *Phys. Lett.* **A155**, 480 (1991).
90. J. Theiler, S. Eubank, A. Longtin, B. Galdrikian and J. D. Farmer, *Physica* **D58**, 77 (1992).
91. H. Tong and K. S. Lim, *Journal of the Royal Statistical Society* **B42**, 245 (1980).
92. H. Tong, *Nonlinear Time Series Analysis* (Oxford University Press, Oxford, 1990).
93. A. A. Tsonis, *Chaos. From Theory to Applications* (Plenum Press, New York, 1992).
94. A. A. Tsonis and J. B. Elsner, *Nature* **333**, 545 (1988).
95. A. A. Tsonis and J. B. Elsner, *Nature* **358**, 217 (1992).
96. A. A. Tsonis, G. N. Triantafyllou and J. B. Elsner, *Nonlinear Processes in Geophysics* **1**, 12 (1994).
97. A. A. Tsonis, G. N. Triantafyllou, J. B. Elsner, J. J. Holdzkom and A. D. Kirwan, Jr., *Bulletin of the American Meteorological Society* **75**, 9; 1623 (1994).
98. B. P. Wilcox, M. S. Seifried, W. H. Blackburn and T. H. Matison, *Chaotic Characteristics of Snowmelt Runoff: A Preliminary Study*. Watershed planning and analysis in action (ASCE, N. Y., 1990), p. 125.

ON
M

The prob
from the
anism ide
typical H
The qual
and the E
underline

1. Introdu

Some of the
related to an
gauge theor
exchange of
in the many

A simple
approximati
case of $f =$
Then there e
incompressib
expected.^{1,2}

Theory o
in usual 3D
standings. I
system of an
coupling the
ton acquires
is indicated
Yang *et al.*⁶
the spectrum